Advances in Aerodynamics

REVIEW

Open Access

Assessing aerodynamic loads on low-rise buildings considering Reynolds number and turbulence effects: a review

Md Faiaz Khaled and Aly Mousaad Aly*

*Correspondence:
aly@lsu.edu

Windstorm Impact, Science, and Engineering (WISE) Research Laboratory, Department of Civil and Environmental Engineering, Louisiana State University, Baton Rouge, USA

Abstract

This paper presents an extensive review of existing techniques used in estimating design wind pressures considering Reynolds number and turbulence effects, as well as a case study of a reference building investigated experimentally. We shed light on the limitations of current aerodynamic testing techniques, provisions in design standards, and computational fluid dynamics (CFD) methods to predict wind-induced pressures. The paper highlights the reasons for obstructing the standardization of the wind tunnel method. Moreover, we introduce improved experimental and CFD techniques to tackle the identified challenges. CFD provides superior and efficient performance by employing wall-modeled large-eddy simulation (WMLES) and hybrid RANS-LES models. In addition, we tested a large-scale building model and compared the results with published small-scale data. The findings reinforce our hypothesis concerning the scaling issues and Reynolds number effects in aerodynamic testing.

Keywords: Atmospheric boundary layer, Low-rise buildings, Reynolds number, Turbulence modeling, LES, Wind tunnel testing, Open-jet testing, Hybrid RANS-LES

1 Introduction

The majority of constructed buildings all across the globe are low-rise [1, 2]. The structural design of different types of low-rise buildings is dissimilar; they are constructed in varying terrain and topography. Apart from very high seismic zones, the strength of buildings is challenged mainly against wind loads. Wind loads have a higher impact on buildings in open terrains, coastal regions, and at the top of hills or plateaus. A building's lateral strength is predominantly challenged because of extreme wind events; however, sometimes, especially for low-rise buildings, severe uplift forces on the building's envelope may cause overall structural collapse. Real wind loads during a storm vary with time and space, which means pressures on a building will fluctuate in magnitude and distribution with time [3]. In aerodynamics, low-rise buildings are considered bluff bodies [4, 5]. Sharp edges, corners, eaves, and surfaces of low-rise buildings experience downstream abnormal pressure gradients, which cause boundary layer separation. This flow separation leads to high negative pressures and strong forces on structural components.

Figure 1 represents the complicated nature of the atmospheric boundary layer (ABL) flow around a low-rise building.

The impact of wind on buildings depends on some complex aspects such as wind velocity, turbulence intensity, integral length scale, nature of topography and surroundings, surface roughness, shape, orientation, among other factors. The images presented in Fig. 2 speak for the catastrophic damages caused by frequently occurring powerful hurricanes in recent years and stress the importance of improving the wind resilience of structures. Over the past three decades, knowledge within the wind engineering field has been advanced by state-of-the-art research studies. Popular methods of ABL simulation include boundary layer open- and closed-circuit wind tunnel experiments, large-scale open jet testing, and computational fluid dynamics (CFD) simulations with their respective advantages and limitations [7–22]. A number of previously conducted wind tunnel experiments, numerical, and full-scale investigations assisted in realizing the flow physics around structures. In engineering practice, aerodynamic loads on buildings are estimated using four approaches: (a) design standards, such as ASCE 7–16, (b) wind tunnel testing, (c) large-scale testing, and (d) numerical simulations (CFD). This paper will scrutinize different aspects of aerodynamic testing and CFD simulations, primarily in relation to the effects of Reynolds numbers (*Re effects*).

Results from several previously conducted wind experiments are discussed in this paper and compared with full-scale data. Discrepancies are observed among full-scale data and model-scale aerodynamic test results, especially, concerning peak pressures. Several publications mentioned Reynolds numbers' inequality (R_e *effects*) and lack of large-scale eddies in small-scale wind experiments as two primary reasons for such discrepancies [7, 23–28]. Particularly, low energy content of large eddies and excessive energy content of small eddies in the incident flow are held responsible for the inconsistency in small-scale experimental predictions [24]. Besides, we aim to highlight the limitations in the design standards to predict wind loads on buildings from previous comparative studies [29, 30]. The past three decades witnessed significant evolution and successful incorporation of computational fluid dynamics (CFD) in wind engineering

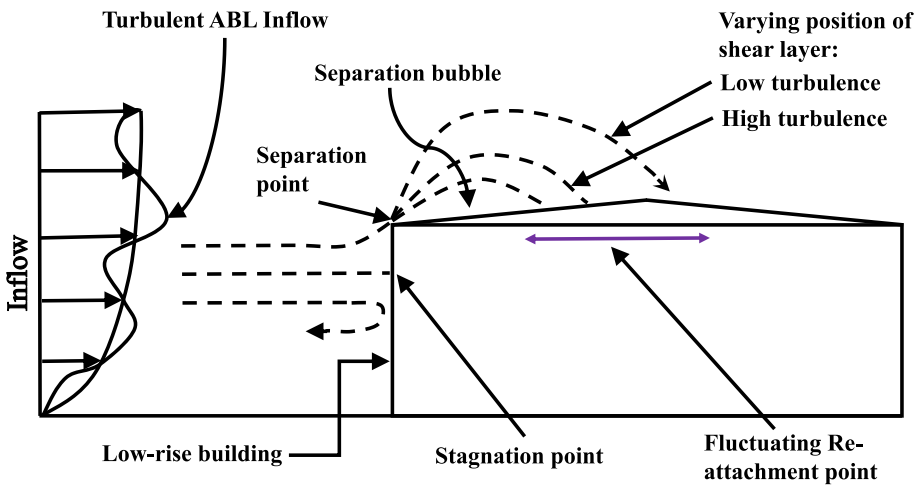

Fig. 1 Wind flow around a low-rise building (adapted from [6])

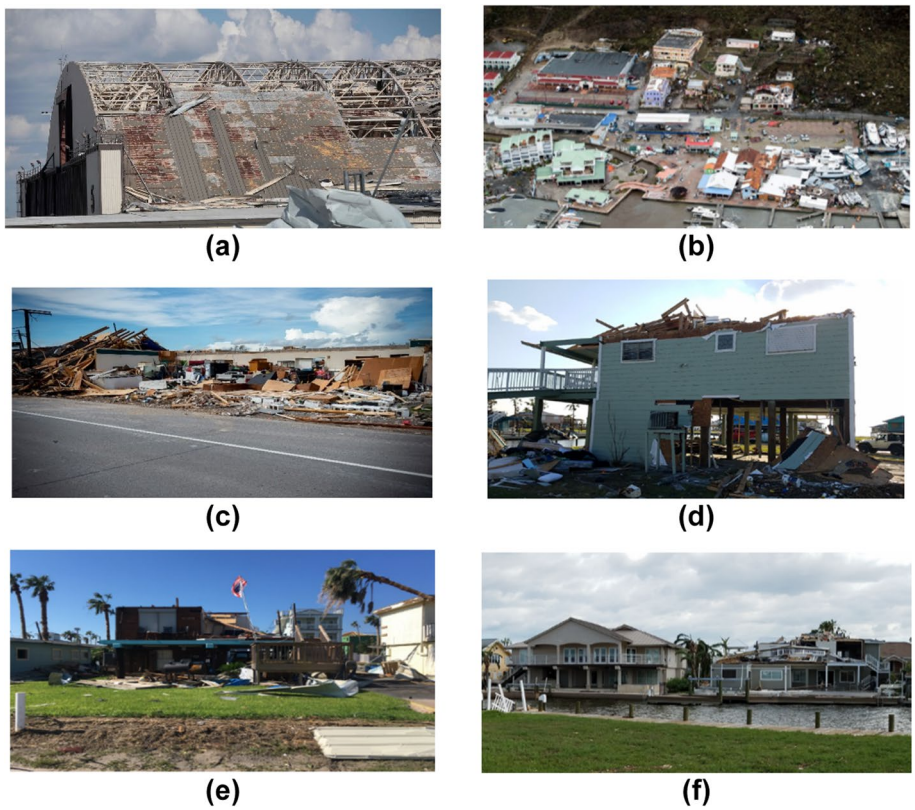

Fig. 2 (**a**) Damage in Tyndall Air Force Base after Hurricane Michael, (**b**) St. Maarten after Hurricane Irma, (**c**) Grand Isle, LA after Hurricane Ida, (**d**) Damage in Holiday Beach Community, (**e**) Structural damage from Hurricane Harvey, and (**f**) Different response of two adjacent buildings in Rockport, TX

applications. The widely embraced CFD techniques are (a) Reynolds-averaged Navier-Stokes (RANS) equations, and (b) large eddy simulation (LES). The issue of treating turbulent flow at high Reynolds numbers using CFD over complex geometries has been a challenge for structural engineers. Two approaches are endorsed and recommended for implementation to address the issue of high Reynolds number. The first approach involves the application of developed wall-modeled large eddy simulation (WMLES) and the second approach integrates RANS and LES to encompass the individual leverage of both methods. Accommodating turbulent flow at high Reynolds number, that is comparable to the full-scale scenario, is a concern in small-scale aerodynamic experiments and to achieve more accurate CFD simulation [31]. Through extensive literature review, we aim to underscore the existing issues in design standards, traditional aerodynamic experiments, and CFD simulations in relation to critical factors such as, R_e *effects*.

To better understand the role of large-scale testing at high Reynolds number, a case study of a cubic model is presented. The experiment is conducted in a state-of-the-art open-jet facility at Louisiana State University (LSU). This open-jet facility enables experiments at larger scales compared to other wall-bounded wind tunnels. A comparison of pressure coefficients for the roof of the cube from the experiment at LSU and previously published data from the Tokyo Polytechnic University (TPU)

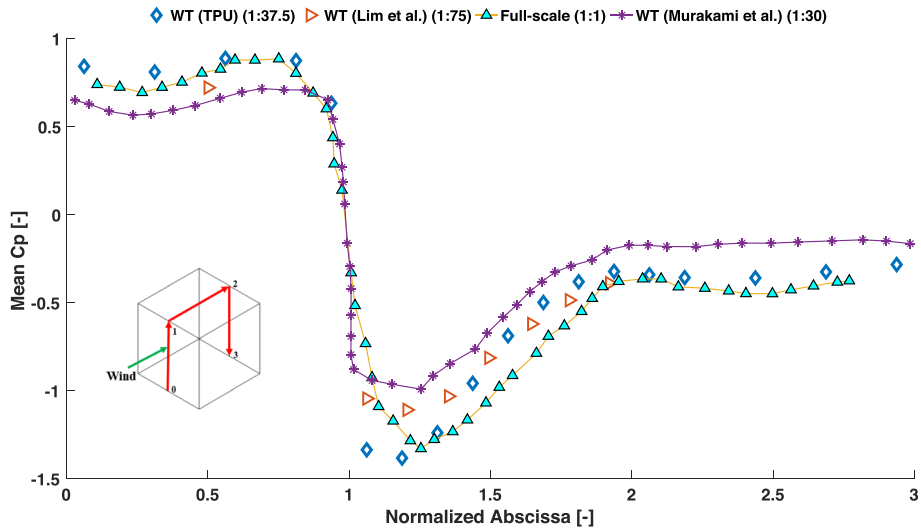

Fig. 3 Comparison of mean surface pressure coefficients from different wind tunnels

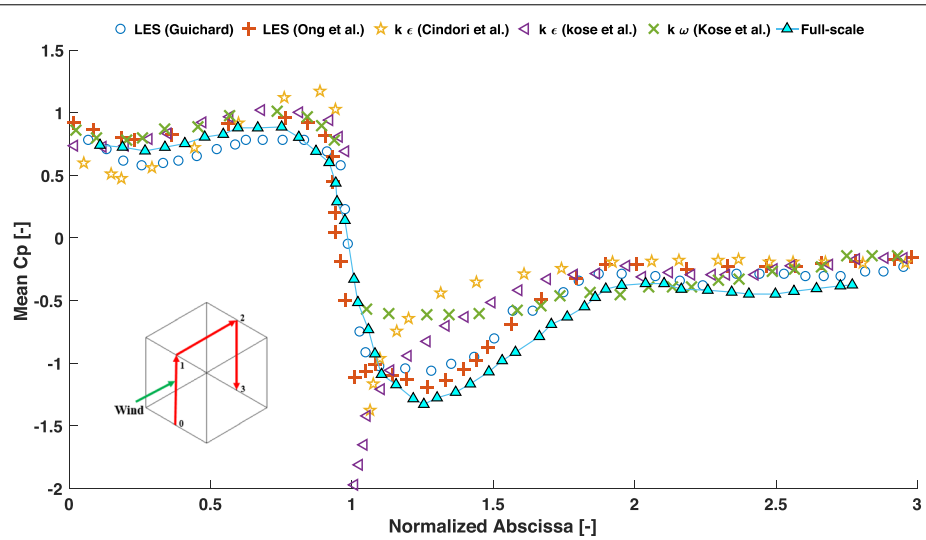

Fig. 4 Comparison of mean surface pressure coefficients obtained using RANS and LES simulations from the literature

are depicted in the form of contour maps towards the later part of the paper. All the pressure coefficients (Figs. 3, 4 and 5, Fig. 10, 11 and 12) presented in this paper are computed by processing the reference dynamic pressures in an identical manner. The reference dynamic pressure is defined as, $q_r = \frac{1}{2}\rho U_r^2$; where, U_r is the reference velocity, which is obtained from velocity measurements at the cube's roof height. It should be noted that this approach is the standard practice to determine pressure coefficients from wind tunnels [32]. The issue of reference pressures in aerodynamic investigations may not be a critical issue for small blockage. In this study, as for the reference pressure, the mean pressure coefficients on the frontal face of the cubic models are checked to see if the results are consistent with regard to the reference pressures

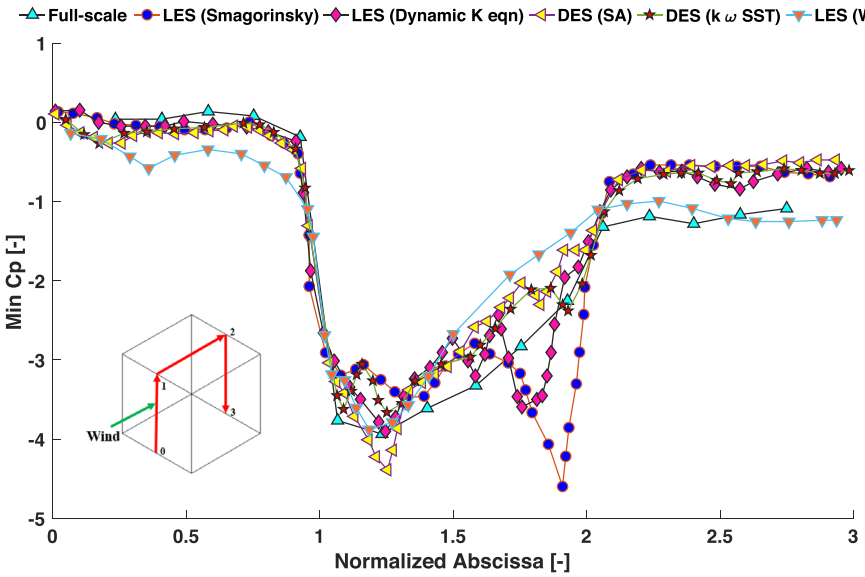

Fig. 5 Comparison of minimum (peak) surface pressure coefficients obtained using LES and hybrid simulations from the literature with full-scale data

during different tests. As long as the corresponding values are consistent in different studies, it becomes reasonable to assume that the reference pressures are not responsible for the differences in the observed results.

Overall, this paper aims to present an extensive review of the existing challenges and promises concerning accurate estimations of surface pressures on low-rise buildings experimentally and computationally in the light of generation of large eddies and *Re effects*. Some limitations, on the experimental side, have already been pointed out in a previous publication [33]. However, this paper attempts to reinforce the review by documenting outcomes of reputed experimental case studies and CFD simulations in relation to the aerodynamics of low-rise buildings. Furthermore, strategies to address the identified challenges concerning experimental and numerical building aerodynamics are introduced. The case study presented in this paper serves as the preamble to exhaustive research into the topic.

2 Effects of Reynolds number

In the early stages of building aerodynamics, there was a widely-accepted notion about the independence of Reynolds number's effects (hereafter referred to as '*Re effects*') for flows with Reynolds numbers higher than $(2-3)\times 10^4$. This underlying assumption acted implicitly as the fundamental basis of the vast majority of the wind tunnel tests with scaled-down models [34]. This idea got acceptance in the early stages as the vast majority of wind tunnel tests primarily focused on simulating the ABL accurately and limited attempts were made to study *Re effects*. Some restricted wind tunnel tests (e.g., [35, 36]) with limited Reynolds numbers' range were at the core of the above-mentioned assumption. On the computational side, an article, [37], investigated the *Re effects* on the mean and RMS values of lift and drag for a square cylinder. LES was used to examine

the effects for a range of $R_e = 10^3$ to $R_e = 5 \times 10^6$. The study reveals that the mean and instantaneous flow structures are not significantly influenced by *Re effects* if $R_e > 2 \times 10^4$; only the small-scale vortical structures are affected by higher Reynolds numbers. However, with research progress, this idea was questioned conceptually and based on experimental data by some pioneers of wind engineering [38]. Further investigation revealed that even mean flow parameters are influenced by *Re effects* for flows characterized with noticeable vortex motions. Whereas, only the fluctuating quantities (e.g., peak pressures) are altered by the *Re effects* for flows without considerable vortex motions (e.g., the wind coming at 45° on a cube).

It is complicated to access the *Re effects* as often the aerodynamic differences are recognized to originate from two more prominent reasons; these are the differences in the upstream flow characteristics (e.g., turbulence intensities and scales) and the mismatch of spectral content between real-world and wind tunnel flows. Several experts have covered the impact of these two factors independently on aerodynamic loads in their research papers. The discrepancies originating from the *Re effects* are often concealed by the differences originating from these two sources. To exclusively assess the *Re effects,* the investigators are directed to ensure two conditions. Firstly, to ensure similar (as closely as possible) upstream turbulence inflow conditions while varying the upstream flow velocities in the tunnel to regulate Reynolds numbers. Secondly, consider the unavoidable effects of mismatch of spectral content between scaled models and full scales while interpreting the results. The inability of wind tunnels to access *Re effects* over a very wide range sometimes makes the investigation of the effects a challenging task. Some wind tunnels only allow varying Reynolds numbers by a factor of 3; varying Reynolds numbers over a higher range than that would require bigger tunnels or aerodynamic testing facilities to account for the instability [34]. Therefore, it cannot be stated with confidence that aerodynamic tests are completely independent of *Re effects* above a certain Reynolds number for any case. The majority of the conclusions presented in this section are for a cubic-shaped building model. The conclusions on the *Re effects* could be different for buildings of different shapes; thus, while conducting any aerodynamic testing, careful attention should be provided on the *Re effects* case by case, without relying on general assumptions. Furthermore, the aerodynamic performance of an obstacle with the inclined roof was investigated at four different Reynolds numbers in the article [39]. A wide range of Reynolds numbers, covering a factor of 12, was executed using CFD simulations. The study reports evident *Re effects* on the local peak values of parameters such as dynamic pressure, turbulence characteristics (viscosity, kinetic energy, and dissipation rate), and vorticity [39]. Similar conclusions are documented in the article [40] that studied *Re effects* on flow behavior within a cluster of buildings located in the lowest part of ABL. Variation of Reynolds numbers is found to influence the turbulence intensities. The core point to be considered is, in real ABL flow, the Reynolds number (R_e) reaches about $R_e = 10^7$, whereas, in most wind tunnels and CFD simulations the maximum R_e that can be reached is about 10^4 [40].

Therefore, the previously endorsed notion of *Re effects'* independency above $R_e \sim (2-3) \times 10^4$ fails to receive total acceptance within the recent experimental and computational wind engineering research community. In order to ascertain how significantly Reynolds numbers, influence surface pressures on low-rise buildings, building

models need to be tested over a much higher R_e range. The ideal strategy would be to test models around R_e~10^7, which is similar to some full-scale range. However, careful attention should be paid to investigate the *Re effects* independently by minimizing the influence of other regulating factors both experimentally and numerically. In order to do that, large-scale testing is highly recommended experimentally as wind tunnels, generally, fail to reach that R_e range. Also, minimizing the computational cost of CFD simulations at high Reynolds numbers is crucial as it is computationally very expensive to examine such effects numerically.

3 Challenges in small-scale aerodynamic testing

The use of aerodynamic testing of small-scale models (geometric scales such as 1:100, 1:500, etc.) to acquire detailed characterization of flow around the built environment has been a common practice in the past four decades. In general, wall-bounded wind tunnel facilities are widely endorsed for such experiments. These tests are effective for a definite number of quantities at a limited number of points and times; moreover, they are only useful for certain operating conditions and a range of problems [41]. With time, questions concerning the accuracy and drawbacks of this technique surfaced. In several cases, small-scale laboratory (SSL) experiments are accompanied by discrepancies when compared to full-scale data. From here on, the phrase 'small-scale laboratory' will be referred to as 'SSL' in this paper. Earlier experiences reveal that the bulk of the experimental errors originate from inaccurate measurements and flow disturbances by the probes [41]. However, the factors instigating differences between full-scale and SSL tests are more complex than that. Review shows that the sources of discrepancies are rooted in but not limited to laboratory arrangement, modeling technique of field condition, target approach surroundings, and technique of taking readings. A large array of turbulent scales generates vortices in the separated shear layer that are responsible for creating strong suction at the leading edges of buildings. This makes the proper duplication of eddies, over the entire wave numbers' range, extremely important [42]. The separation of smaller and larger wavelengths of velocity variation in the frequency domain, for inflow with high Reynolds numbers, is higher than that for small-scale wind tunnel inflow at low Reynolds numbers. This is a fundamental deficiency of SSL experiments in modeling ABL flow [42].

The importance of comparing full-scale measurements and SSL experiments of wind pressure on low-rise buildings has been addressed by several researchers over the years [43–48]. Small-scale wind tunnel experiments generate the actual global nature of wind and pressure like those found from full-scale measurements. But, when it comes to reproducing properties related to local pressure, some discrepancies between model and full-scale testing are evident [49]. Despite being expensive, full-scale tests are important for validating experimental results as such tests reveal the actual aerodynamics around buildings. Figure 3 compares the mean pressure coefficients obtained from three different wind tunnel experiments with full-scale measurements [50, 51]. Variability is observed even in the case of mean pressure coefficients. Figure 3 shows that none of the wind tunnel results precisely overlap with the full-scale data points over the entire vertical ring. The coefficients for full-scale surface pressures for the cubic model are processed in the method proposed in [32]. Figure 3 shows that the TPU wind tunnel offers

better accuracy on the windward side, roof, and leeward side compared to the other two wind tunnels. The apparent differences among the wind tunnel observations could be the result of a wide range of factors such as, but not limited to, variations in inflow features, Reynolds number, relative roughness, blockage effects, etc. The uncertainties related to the experimental setup were not reported in the TPU database; therefore, it becomes challenging to estimate other uncertainties that could possibly produce differences in results [52]. However, considering the available information, the improved prediction of mean pressures might be attributed to the presence of a higher Reynolds number in the TPU wind tunnel inflow (Table 1). However, all three wind tunnel results are characterized by faster pressure recovery leading to shorter reattachment length, which leads to the mismatch of pressure coefficients on the roof. The shortcomings of such experiments (Fig. 3) to predict roof pressures reinforce the need for further research using advanced experimental and computational techniques. Besides, this also emphasizes the importance of standardizing testing protocols for aerodynamic testing.

Furthermore, the review shows that between full-scale and model-scale perfect duplication of fluctuating pressure coefficient is not guaranteed by intricate simulation of variables, e.g., turbulence intensity, mean velocity, etc. Moreover, fluctuating pressure coefficients show a considerable amount of scattering [55]. It is reported that for mean,

Table 1 Flow characteristics in different experiments

Case	Features	Values or parameters used
Richards et al. (Silsoe) [45]	Building height, H_{ref} (m)	6
	Scale (w.r.t. Silsoe)	1:1
	U_{ref} (m/s)	9.52
	I_u (%)	0.193
	Reynolds number	4.1×10^6
	Sampling rate; time	Pressure: 25 Hz; 20 minutes
Lim et al. [50]	Building height, H_{ref} (m)	0.08
	Scale (w.r.t. Silsoe)	1:75
	U_{ref} (m/s)	3.49
	I_u (%)	Excess of 25%
	Reynolds number	2×10^4
	Sampling rate; time	Velocity: 2 to 10 kHz; 60–120 seconds Pressure: 50 blocks of 4096 samples at a rate of 2 kHz.
TPU WT [53]	Building height, H_{ref} (m)	0.16
	Scale (w.r.t. Silsoe)	1:37.5
	U_{ref} (m/s)	8.274
	I_u (%)	25
	Reynolds number	1.14×10^5 (Approx.)
	Sampling rate; time	Pressure: 500 Hz; 18 seconds for each sample. Was sampled 10 times.
Murakami et al. [54]	Building height, H_{ref} (m)	0.2
	Scale (w.r.t. Silsoe)	1:30
	U_{ref} (m/s)	–
	I_u (%)	–
	Reynolds number	7×10^4
	Sampling rate; time	–

low, and moderately high peak pressure coefficient results acquired from wind tunnel and field measurements are in good agreement [56]. But, for high peak pressure coefficients, some discrepancies between results from the two sources were observed. The wind tunnel test underestimated high peak pressure coefficients. The difference in Reynolds number might be responsible for the discrepancy. Eddies with higher frequencies, observed in full-scale, are suppressed in the wind tunnel because of viscous dissipation [56]. This type of comparison is beneficial for validating wind tunnel data. However, the results of high peak pressures from the wind tunnel should not be considered for codification due to the discrepancies discussed earlier. Similar inferences concerning peak pressures for model-scale and full-scale models are reported in [30, 57–62]. Although full-scale tests are more accurate, sometimes these tests are also accompanied by some difficulties, which may result in inaccurate measurement [63]. In full-scale testing, the cost and time associated with the construction of models, installation of necessary apparatus, and retrieving desired results are relatively higher. Besides, some factors such as lack of adequate control on the desired inflow, and requirements of advanced data acquisition systems add to the difficulty of full-scale field studies. Such a highly expensive form of aerodynamic investigation cannot be repeated for different structures and shapes. However, this form of testing is the most reliable source for validating results from other techniques. Large- and full-scale testing can be considered a powerful tool that will augment the understanding of results obtained from other aerodynamic experiments and numerical simulations [64]. In the cited study, inconsistencies are observed while comparing mean pressures from full-scale and smaller laboratory models; this might be attributed to the difference in Reynolds numbers and the formation of separation bubbles on sharp eaves. Such observed discrepancies, concerning mean and fluctuating pressure coefficients, are attributed to (1) improper simulation of turbulence intensity, (2) inappropriate detailing of the model in the wind tunnel, (3) stationary state of wind flow, and (4) influence of Reynolds and Jensen number [65]. The studies [59, 61] report better agreement with the increase in Reynolds numbers. Moreover, a comparison of results from six well-known wind tunnel laboratories revealed a significant scattering of 50th percentile peak pressures in [27]. Inadequate sample size, difference in reproducing terrain characteristics, inconsistencies regarding peak wind effects, and the impact of violating Reynolds numbers' similitude law in the laboratory are identified as possible reasons for such scattering in addition to some other factors.

It can be stated with certainty that the proper generation of wind speed, turbulence intensity profiles, and spectral characteristics is important for evaluating accurate aerodynamic loads on structures [33, 66]. The dissimilarity of Reynolds numbers between experimental flow and real wind is considered as one of the leading causes of deficient generation of turbulent eddies over the entire frequency range [33, 42]. Furthermore, the differences in turbulence spectra are responsible for the large variations in aerodynamic loads when cases from different wind tunnel experiments are studied [67]. All these aforementioned issues lead researchers towards alternate methods for aerodynamic testing. Large-scale wind tunnels and open-jet facilities are becoming more appreciated in the wind engineering community to offset the shortcomings of SSL experiments. We endorse the concept of open jet experiments more than large-scale wind tunnels because in the open jet the flow is generated without physical boundaries. Such type of

experimental set-up can generate wind flow around buildings that offers better representation of real-world wind flow. Large-scale wind tunnels can test larger models, but such facilities are with boundaries that affect the near-wall wind flow. Besides, such facilities are deficient in generating large eddies that are responsible for peak aerodynamic loads. The blockage requirements of wind tunnels do not apply in case of open jets as meaningful results are obtained in open-jet facilities with large-scale models. The contents of this section serve as the motivation for the experimental study conducted in the paper.

4 Concerns about the ASCE provisions

Different versions of the ASCE standard have been used by engineers over the years and are considered as guidelines for aerodynamic loads' estimations on low-rise buildings. The standards were primarily developed based on SSL experiments conducted about three to four decades ago [68] and went through subsequent analysis, examination, and improvement in stages [29, 69, 70]. This section attempts to present the acceptability of the ASCE standards' provisions in comparison to more advanced aerodynamic testing. A comprehensive dataset of aerodynamic loads on low-rise buildings was developed by the collaborative efforts of the University of Western Ontario (UWO), Texas Tech University (TTU), and the National Institute of Standards and Technology (NIST). The involved institutions attempted to employ state-of-the-art wind tunnel testing of that time. The study compared the provisions in ASCE 7–02 with those from the aerodynamic dataset. The paper concludes that ASCE 7–02 underestimates the point pressures but predicts area-averaged loads reasonably well [71].

Likewise, comparisons between the full-scale evaluation of dynamic pressures and wind loads specified in ASCE 7–05 show that the prevailing design wind load provides an inaccurate prediction of response which may give way to underestimation of the effects of design wind speeds [72]. Another similar study [30] identifies higher discrepancies in magnitudes for peak pressure coefficients compared to the mean values. The cited study shows that measured and predicted extreme peak pressures on the windward side and roof are higher than those found from ASCE 7–10 [73]. Moreover, it was concluded that ASCE 7–10 fails to provide a conservative design in the case of flat-roof low-rise buildings [61]. Similar observations are reported in [74, 75] when pressure coefficients from ASCE 7–10 and field measurements are compared. The study [75] infers that ASCE 7–10 significantly underestimates the pressure coefficients, with a relative error of 41%, when compared to TTU field measurements. The dependence on wind tunnel data is cited as a possible reason for this underestimation. The investigation of area-averaged surface pressures stipulated in ASCE 7–10 by [76] contributed to the improvement of pressure coefficients in ASCE 7–16 (chapter 30).

In ASCE 7–16, the roof pressure coefficients have been updated following state-of-the-art wind tunnel testing procedures [77]. Another recent study [62] conducts cross-comparisons among full-scale field measurements, wind tunnel results, and stipulations in design codes and standards. The study confirms that the net pressure coefficients, from full-scale and model-scale measurements, on roof overhang are lower than those stipulated in ASCE 7–16; in other words, ASCE 7–16 provides conservative pressure estimations in corner zones of a roof overhang. The study [78] concludes that despite considerable improvement in mean and peak pressures on the overall roof, ASCE 7–16

cannot provide a conservative estimate of aerodynamic loads for certain shapes of low-rise buildings. Furthermore, for roofs with large spans and low slopes, peak pressure coefficients stipulated in the ASCE 7–16 are found uneconomical and conservative when compared with the corresponding experimental data from a 1:400 scale wind tunnel model [79]. Whereas, another study [80], where large-scale aerodynamic testing of a similar building model was conducted, concludes that the peak loads are underestimated in the ASCE 7–16 compared to their observations. Therefore, the peak loads in the ASCE 7–16 are found conservative when compared to wind tunnels' findings, and the same are found inadequate when compared to large-scale open-jet results. This demonstrates the need to create a reliable and accurate basis to formulate the stipulations in the design standards in a way that it can predict the true full-scale behavior of buildings under wind.

5 Application of CFD in wind engineering

CFD is well established within the aerospace industry as the experts in that field have been able to accurately capture the fluid flow numerically. On the contrary, building aerodynamics is characterized by flow separation, flow reversal, and formation of vortices. In the past, the accuracy of CFD simulations to predict flow around bluff bodies has been questioned and argued upon, even for simple shapes of buildings [50, 81–85]. Nevertheless, it should be clearly stated that the flow around streamlined objects is no less complicated. Generally, turbulent flow is dealt with in three different ways; the methods are Reynolds-averaged Navier-Stokes equations equipped with a turbulence model, direct numerical simulation (DNS), and LES [69]. The pros and cons of the commonly used turbulence closures in building aerodynamics are summarized in a recent publication [86]. The complex flow features around buildings pose numerical challenges, which inhibited the rapid growth of CFD in structural engineering [41]. Some characteristics of such flow scenarios impede strong acknowledgement of CFD within the wind engineering community; these are [69], (1) large turbulence, (2) large Reynolds number, (3) three-dimensional flow field, (4) characteristics associated with the bluff body, and (5) vortex shedding. About a decade ago, the AIJ researched the improvements of CFD in estimating wind impact on buildings numerically [87]; the notable improvements were: (1) replicating inflow turbulence and (2) modeling of flow separation over bluff bodies along with vortex shedding. It is rational to suppose that the vortices present in the incident flow interact with the structure and undergo deformation; consequently, unsteady loads are experienced by buildings' surfaces. Quantifying the turbulent structures in the incident flow with CFD and identifying how aerodynamic loads are created from those structures can have a far-reaching influence in building aerodynamics [50].

This emphasizes the importance of validation as a fundamental step for most CFD problems in wind engineering. Employing wind tunnel tests for validation purposes is very common in wind engineering [41, 88]. However, wind tunnel tests are not recommended to be considered as the benchmark since some discrepancies have been documented earlier in the literature. Researchers from the WISE research group at LSU will focus on comparing the CFD results with state-of-the-art large-scale testing in their future endeavors. Both CFD simulations and experiments should be able to replicate full-scale flow behavior; therefore, the primary target should be to validate using

full-scale data. The complexities in building aerodynamics originate from flow features such as flow separation and reattachment near buildings' edges at high Reynolds numbers. The numerical settings that are suitable to capture such features at high Reynolds numbers can be considered appropriate for building aerodynamics. LES is considered to be well suited for investigating the flow around low-rise buildings as it resolves the large-eddies (that are directly impacted by the boundary conditions); LES models small-scale eddies that are considered to be more universal [89]. Successful applications of LES to model flow separation were reported in several previous studies [90–93], which makes it suitable for investigating wind flow around low-rise buildings.

5.1 Large eddy simulation (LES)

Significant contributions over the past 4 decades have led LES to a level of maturity, where it has started gaining acceptance to treat industrial turbulent flow problems [82, 94, 95]. This becomes evident by observing the number of publications on LES that has increased tenfold since 1980. The focus of the research community has shifted from developing the theoretical part to treating real-world industrial problems. The developments, till 2010, and challenges, associated with growing needs, are reviewed in the article [94]. The mere usage of LES does not guarantee the qualitative and quantitative accuracy of results [96]. Both DNS and LES can be useful CFD simulation techniques to simulate the unsteady flow. However, LES is preferred over DNS as the latter takes more computational time and storage [97]. DNS is prohibitively expensive but conducted in some benchmark studies to validate future CFD simulations with models of lower accuracy [98]. In LES, eddies larger than the grid size are resolved, whereas eddies smaller than the grid size are modeled using subgrid-scale (SGS) models [99]. Like other CFD simulation models, LES is sensitive to numerical and physical parameters used in the simulations. Factors such as choice of SGS model, length of the computational domain, type of filtering, meshing strategy, time-step, sampling time, numerical schemes, etc. could influence LES results significantly, depending on the flow problem. Unlike RANS, very few parametric studies are conducted, and limited attempts are observed in literature while searching for optimal simulation guidelines. A study, [100], attempted to investigate the sensitivity of some influencing parameters, such as the SGS model's selection and inflow generation technique, in the case of wind-flow around an isolated building with LES. Readers are directed to the cited article for more details about their findings. Moreover, the effects of numerical schemes and meshing strategies on flow over a similar geometry were examined with open source finite volume code (OpenFOAM) in the paper [101]. In OpenFOAM, notable differences were not observed for different numerical schemes. Furthermore, the article [102] is one of the very few studies that explored the influence of spanwise grid resolution on surface pressures, vortex shedding in the wake, and shear layer separation around a bluff body. More research is required for detailed conclusions on this topic. Moreover, the inflow generation technique is identified to influence flow around buildings including several other factors. Exhaustive review of the synthetic turbulence approach is beyond the scope of this paper. The cited studies [103, 104] extensively review the pros and cons of synthetic turbulence generation (STG) and precursor simulation techniques in detail. Accurate pressure prediction with LES requires proper inflow turbulence boundary conditions

[105–107]. The available turbulence generation techniques for LES are broadly classified into three categories, which are (a) precursor database, (b) recycling method, and (c)) STG [95, 105, 108–113]. STG techniques entail the addition of artificial fluctuations to a given mean profile, which introduces advantages such as (a) computational efficiency, (b) convenient implementation, and (c) highly versatile due to its dependence on local variables [114]. The gradual development of STG was possible because of some remarkable research endeavors, which are listed in Table 2.

Notwithstanding the above-mentioned advantages, the STG approach has some drawbacks as well. A fundamental limitation is the inability to generate divergence free velocity field. If the generated velocity field is not divergence free, then LES will initiate considerable pressure fluctuations near the inlet to maintain divergence free velocity field inside the domain. If divergence free velocity field can be introduced at the inlet, then the simulation will undergo lower pressure variations near the inlet, resulting in lower computational costs. In order to address this issue, intelligent strategies to generate desired fluctuating velocity fields are proposed in a few studies [113, 125–128] besides the articles cited in Table 2. Nevertheless, STG offers higher computational efficiency. The Random Flow Generation (RFG) method is used by most commercial software [129]. Since the turbulent spectra in the lower portion of the ABL are different from that of Gaussian spectra, this RGF technique is not compatible with generating inflow in wind engineering. To replicate target spectra the discrete

Table 2 Notable scientific contribution to the evolution of STG

Contribution	References
• The fundamental idea of STG was introduced in 1970. • Described velocity field as the summation of Fourier modes. • The amplitude and phase of the modes are random.	[115]
• The method introduced in [115] was improved later in this study. • Proposed an isotropic turbulence generation technique. • Produced turbulence with target root mean square value, and zero mean value.	[116]
• One of the embryonic limitations of the STG approach was the need for longer length before developing the characteristics of realistic turbulence. • Proposed improvement introduced space correlation between fluctuations.	[110]
• The problem was alternately addressed by employing goniometric functions so that target fluctuations can be imposed, and desired spectral distribution can be obtained.	[117, 118]
• Introduced inflow for noise modeling in case of free jet flows.	[119]
• Random flow generation is proposed for turbulent shear flows. • Spatial inhomogeneity and anisotropic nature of stresses. • Accepts a priori Reynolds stress tensor, length, and time scale as input.	[120]
• The cited studies made improvements over the previous four studies. • Enhanced anisotropic features and turbulence spectral content.	[112, 117]
• Similar approaches were proposed recently for aerodynamic applications. • Anisotropic and inhomogeneous features are ensured in the flow generation. • Suitable for RANS, LES, and DNS applications.	[121, 122]
• STG involving digital filtering method was introduced in the cited study.	[107]
• Pioneering articles proposing STG techniques that satisfy divergence free condition: • By superimposing harmonic functions [120]. • The method proposed in [120] was improved by employing Von Karman spectrum instead of Gaussian model [112]. • The velocity potential for divergence free condition was derived and the numerical solution was computed [123]. • A similar method was proposed in that demonstrated reduction in pressure variations [124].	

Table 3 Findings concerning LES in the literature for low-rise buildings

Summary of findings	Ref.
• The mean and root mean square (rms) pressures concur well with those from the experimental data for a half height cube with turbulent inflow using LES. • Underestimation of peak pressures near the edge is observed. • The identified reasons are shorter duration of data collection, small integral length scale, and numerical damping caused by adoption of upwind scheme.	[111]
• Mean and peak surface pressures on single-span greenhouse buildings of different roof slopes and radius of curvatures were predicted using LES. • The observations were later compared with previously done RANS simulations ([131]) and corresponding wind tunnel experiments. • Improved mean pressures are observed from LES compared to RANS simulations. • The mean pressures from LES closely agree with those from the experiments. • The peak pressures also concur with the experimental counterparts with some localized discrepancies. • Overall, LES was concluded to produce reasonable peak pressures as well.	[132]
• LES can produce accurate unsteady aerodynamic pressures on isolated buildings when realistic wind flow is generated near the buildings' location. • The proposed RFG technique can produce realistic inflow at lower computation cost compared to precursor simulation, recycling, and other techniques. • The turbulence intensity at the inlet needs to be adjusted to obtain desired intensity at the zone of interest.	[52]
• LES is employed to ascertain the mean and peak pressures on a 1/200 model of a gabled-roof low-rise building. • Later, the obtained results were compared with previously conducted wind tunnel experiments. • The mean surface pressures had better correspondence to wind tunnel counterparts, whereas the peak pressures were underestimated by LES simulations.	[133]
• LES was employed on a 1:1 scale of the TTU experimental building to study the mean and peak pressures. • The mean surface pressures were in desirable agreement with the full-scale counterparts. • Also, highly encouraging peak pressures were obtained from LES with minor deviations from full-scale measurements. • This study also contributed to the best practice guidelines of CFD LES for wind engineering applications.	[75]
• Flow behavior around low-rise buildings of different shapes was investigated using PIV wind tunnel experiments and 3D LES. • LES can reproduce time-averaged, RMS velocities and vortices that are consistent with the experimental findings depending on the geometric shapes of roofs. • LES predictions for flat roofs are more accurate compared to roofs of complex geometries.	[134]
• Mean pressure distributions on gable-roof low-rise buildings of variable roof pitches were investigated. • Higher suction was observed for lower roof pitch; in other words, flat roofs are more vulnerable during powerful windstorms. • LES has better predictive ability of near-structure wind field and mean localized surface pressures compared to RANS; however, it is obtained at the expense of 80 times higher computational cost.	[135]
• The cited study presented some best practice guidelines for RANS and LES simulations concerning the following: numerical settings, turbulence model, numerical discretization, and computational domain. • LES is essential for accurate estimation of wind loads and predicting peak values.	[87]
• The treatment of flow over complex geometries and/or treating flow of high *Re* are identified as challenging tasks for LES.	[94]
• The cited study reviewed the prominence of LES in investigating flow around buildings till 2008. • For a wide range of avenues of building aerodynamics, including estimation of surface pressures, LES has demonstrated to produce reasonable results based on wind tunnel experiments. • However, to establish LES as a stand-alone tool, the findings need to be validated with full-scale measurements.	[95]

random flow generation (DRFG) was proposed. The DRFG technique was improved to obtain better compliance with target spectra [105, 130]. These techniques are within the category of STG, which is computationally more efficient than the other two methods. Since this paper deals with the estimation of surface pressures on low-rise buildings, Table 3 presents the core findings of some notable research papers for such buildings employing LES.

Table 4 Available information on different simulations

Case	Properties	Values/parameters used
Guichard [52]	Y+ (Reduced scale)	50
	Building height (m)	0.1 (1:400)
	Turbulence model	LES (WALE SGS)
	Velocity at roof height (m/s)	7
	Turbulence intensity at roof height	23%
	Time	0.55 minutes
	Time-step	0.001 seconds
Ong et al. [32]	Roughness length (m)	0.01 (Open terrain)
	Building height (m)	6
	Turbulence model	LES (Smagorinsky) LES (Dynamic K Eqn) DES (Spalart-Allmaras, SA) DES ($k-\omega$ SST)
	Velocity at roof height (m/s)	5.68
	Turbulence intensity at roof height	20%
	Time	25 minutes
	Time-step	0.01 seconds
Cindori et al. [138]	Terrain type	Sub-urban
	Building height (m)	0.202
	Turbulence model	RANS ($k-\boldsymbol{\epsilon}$)
	Velocity at roof height (m/s)	13.48
	Turbulence intensity at roof height	20%
Köse et al. [139]	Building height (m)	6
	Turbulence model	RANS (Standard $k-\boldsymbol{\epsilon}$) RANS ($k-\omega$ *SST*) ILES (Implicit LES; no SGS model: Cs = 0)
	Velocity at roof height (m/s)	9.52
	Turbulence intensity at roof height	20% [45]
	Cell-count	1.2 million
	Time (Averaging)	2 minutes
	Time-step	0.01 seconds

Besides, estimation of surface pressure coefficients is sensitive to turbulence models as well. Surface pressures, predicted using LES, were compared with experimental results and field measurements in a wide range of studies. In several studies, mean and peak pressure coefficients from LES are reported to be in harmony with field measurements and experimental data [97, 136, 137]. Figure 4 offers a similar presentation style (as in section 3) for comparing mean pressure coefficients to full-scale measurements. In this figure, mean pressure coefficients on the vertical ring of a cube are reproduced from the data found in the literature [32, 52, 138, 139]. The numerical settings and simulations' details of studies for Figs. 4 and 5 are presented in Table 4.

Figure 4 demonstrates the superior performance of LES compared to RANS even for mean pressure coefficients' predictions on the building's roof. RANS and LES reveal similar mean values for the windward and leeward sides. However, distinct differences are observed on the roof, where the flow physics is accompanied by flow separation and reattachment. The reattachment length predicted by LES is close to full-scale measurements, leading to similar mean pressure coefficients on the roof. This comparative study

of mean pressure coefficients from the literature adds to the eligibility of LES in building aerodynamics. However, LES results (Fig. 4), from the two sources, show some deviations from full-scale coefficients on moving downstream on the roof.

Furthermore, Ref. [137] reports discrepancies in the standard deviation of estimated pressure coefficients, and Ref. [111] documents the underestimation of peak pressure coefficients. The study in Ref. [134] concludes that the numerical results from LES showed good agreement with the PIV experimental data based on statistical analysis. The same study reports better performance of LES for flat roofs compared to more complex roof shapes. Furthermore, the cited article [75] reveals that mean pressure coefficients from LES are comparable to the full-scale measurements when an appropriate inflow generation technique is employed. Peak pressures are well reproduced with small discrepancies by LES; however, there is ample scope of improvement and research in the prediction of peak pressures using LES. The notable influence of mesh size and turbulence intensity on extreme pressures' predictions is confirmed in the study [32]. Figure 5 compares peak pressure coefficients on the vertical ring obtained from different transient CFD simulation cases (from literature) with full-scale data [140]. In the cited study, the full-scale peak pressure coefficients were obtained by normalizing with maximum observed dynamic pressure. In this study, the collected full-scale data are multiplied by a factor of 3.21 to make a fair comparison and to remain consistent with the commonly used aerodynamic pressure coefficients' normalizing technique. In the present study, all pressure coefficients are computed by normalizing with dynamic pressure obtained from the mean wind velocity $\left(\frac{1}{2}\right)\rho U^2$. LES cases produce encouraging performance with some discrepancies on the roof and the leeward side. Higher discrepancies are observed near the downstream end of the roof. Results reveal a degree of sensitivity to the employed SGS model. However, LES with the WALE SGS model generates more accurate peak values on the leeward side.

The study [141] reports the possible influence of SGS models on results especially for flows with high Reynolds numbers. Furthermore, pressure coefficients were compared after employing eight different SGS models; the selection of SGS models is not reported to produce accurate predictions of mean and peak pressure coefficients. The recommended meshing strategy in the cited paper produced the least errors (in the order of 20%) when compared to experimental measurements. However, the influence of SGS models on surface pressures needs to be investigated more after analyzing the empty domain results reported in [86]. Comparing LES results with experiments quantitatively has gained acceptance recently. To rely on LES predictions with higher confidence, several recent studies compared LES predictions with some benchmark experiments quantitatively [142–144].

In addition, LES with coarser near-wall grids produces inaccurate Reynolds shear stress in the near-wall region as SGS models fail to perform accurately on such grids [145, 146]. Employing finer near-wall grid refinement could be one way to address this issue; this would allow the grid to resolve smaller eddies that produce stresses. However, such an arrangement can significantly increase the total cell count as the cell sizes become remarkably smaller compared to the boundary layer thickness for cases with high Reynolds numbers. Consequently, the computational expense of such wall-resolved large-eddy simulation (WRLES) cases reaches closer to those of DNS simulations

[147]. Furthermore, another persistent challenge with LES applications is its inability to resolve high-frequency small fluctuating eddies. By definition, LES resolves large eddies and models smaller eddies with SGS models; in other words, the small eddies remain unresolved or under-resolved in most real-world LES applications. Adopting coarser grid refinement is considered one of the key reasons behind this commonly observed phenomenon. This results in leakage of energy in the high-frequency end of turbulence spectra, often due to viscous dissipation. One way to address this concern is employing a higher density meshing arrangement throughout the domain or near the zone of interest. Either way, the result is the consumption of higher computational resources. This creates the importance of researching advanced modifications to LES so that even denser meshing arrangements can be treated faster. Employing advanced SGS models can augment LES performance as the task of such models is to account for the under-resolved small-scale structures and draw adequate energy from the flow [148]. We researched this topic using an empty domain and reported encouraging conclusions [86]. Some other studies propose advanced SGS models to reduce the errors associated with modeling small eddies [149–151]. Besides, the point a CFD engineer needs to ponder over before adopting a specific technique, such as LES, is to anticipate how that model would perform for the particular flow problem under consideration. It is well known that the success of CFD applications varies significantly depending on the flow problem. In many applications, the truncated high-frequency small scales with low energy are considered inconsequential. However, such structures provide precise information about the development of large-scale structures in turbulent flows [148]. For building aerodynamics, sometimes the peak loads cause failure in low-rise buildings; therefore, it becomes important to decide on the suitability of a model by inspecting the ability to accurately evaluate peak loads. Accurate peak loads are produced experimentally or numerically by ensuring large eddies in the inflow with adequate energy [33, 75]. In such problems, reproducing accurate low-frequency fluctuations may be sufficient. However, research should continue to improve the under-resolved or unresolved eddies in LES applications. The perfect solution for such problems would be to reproduce eddies over the entire frequency range at a reasonable computational cost, which acts as a motivation for new research.

This section presents multiple reasons behind the higher approval of LES in the structural/wind community with some existing shortcomings. Until now, LES has been unable to entirely replace RANS models when the primary objective is to predict only mean aerodynamic loads; this is because of higher computational cost, lack of adequate best practice guidelines, and complexity of simulation in LES [152]. Moreover, issues related to the selection of filtering techniques, closure modeling, and near-wall treatment are identified as the major impediments for industrial CFD practitioners [94]. We will attempt to present some alternate strategies to address the limitations of LES in subsection 5.2. This section presents the encouraging capabilities of LES along with its limitations and avenues of improvement for wind engineering applications.

5.2 Strategies to treat flows at high Reynolds number

Despite producing encouraging results, the computational expense associated with LES for flow problems at high Reynolds numbers is a major impediment in the total dominance of LES. This section presents a review of some innovative simulation strategies

that have produced promising results to model flow separation and reattachment at high Reynolds numbers. The literature review covers articles from fields related to fluid mechanics, not only limited to civil engineering. Two methods are proposed that are used to treat similar problems in other disciplines. The first approach employs developed wall-modeled LES (WMLES) and the second approach involves the unification or hybridization of RANS and LES methods.

5.2.1 Wall-modeled LES applications

The most widely accepted approach to treat near-wall problems is modeling the layer close to the wall [153, 154]. Wall modeled large eddy simulation (WMLES) delivers to make LES computationally more affordable by reducing finer near-wall cell requirements [89]. The wall functions for LES differ from those used in RANS. Larger grid spacings allow the use of higher time-steps that makes transient simulations hundreds to thousand folds faster and concurrently, maintaining a stable courant number. Moreover, WMLES addresses the issue of inaccurate near-wall shear stress prediction by SGS models with coarser grids. With WMLES, total shear stress is augmented by employing modeled boundary conditions in the region close to the walls. Wall models receive more accurate LES information, in the case of WMLES, compared to wall functions in RANS models. Additionally, WMLES are less sensitive to issues such as grid-induced separation and mismatch of logarithmic layer [155]. It is important to highlight the endeavors to develop an improved SGS model that employs a length scale regardless of the grid. This new SGS model is capable to predict mean and turbulent flow features more accurately, reducing the dependence on wall models [156, 157]. Although these developments have shown promise to produce accurate and affordable results with LES at high Reynolds numbers, further research is required for validation for complex structures and higher Reynolds numbers. Similarly, the study [89] concludes that WMLES can reasonably predict mean and turbulent flow features with a coarse grid; the study investigated flow separation and reattachment on NASA wall-mounted hump.

Moreover, an approximate equilibrium wall-boundary condition was introduced to model the near-wall flow behavior [153]. Over the years, several experts have introduced modifications to this model in Refs. [154, 158–160]. A wall-model for LES was proposed in [161], which performs satisfactorily for both equilibrium and non-equilibrium flow problems at any Reynolds number. Integrating wall modeling with the synthetic eddy method was demonstrated to be competent in reducing the computational cost for two specific cases of high Reynolds numbers [162]. It performed efficiently in representing the near-wall flow behavior in complex flows accurately. Also, the inlet boundary can be positioned closer to the zone of interest in the domain, leading to a further reduction in the computational demand. Integrating the synthetic eddy method with wall-modeled LES was found to perform very well for complex flows at high Reynolds numbers. A similar strategy was followed in a recent study [86] to compare the computational efficiency of LES with different Subgrid Scale (SGS) models. The study demonstrated the superior efficiency of the wall-adapting eddy viscosity (WALE) SGS model while producing empty-domain flow characteristics of higher accuracy. Accurate empty domain flow features are crucial for accurate peak loads' estimation. However, further research

is required to observe the performance of SGS models, with pure LES cases, to predict more accurate peak pressures.

5.2.2 Hybrid RANS-LES techniques

Earlier discussions on RANS and LES indicate the supremacy of LES that facilitates accurate flow simulations. The majority of structural engineering applications involve wall-bounded turbulent flows; the complication is LES becomes remarkably expensive (computationally) while treating such flows (almost as expensive as DNS) [163]. LES demands prohibitive grid resolution to deal with near-wall eddies within high Reynolds number boundary layers. A justifiable approach is to devise hybrid RAN-LES methods; however, it has been surprisingly challenging to develop reliable hybrid methods for different flow problems. The fundamental difference between the RANS and LES equations is responsible for the dubious performance of hybrid methods. LES equations are capable of capturing fluctuations, whereas RANS equations fail to deal with fluctuations [163]. In this method, the RANS equations are used near the wall and LES filtered Navier Stokes equations are employed away from the wall. Several techniques have been proposed to switch between RANS and LES. The Spalart-Allmaras (SA) turbulence model used the distance from the wall as a criterion to switch between the RANS-LES in detached eddy simulation (DES); the SA model was later extended into other two-equation turbulence models [164]. The Hybrid RANS-LES models are suitable for complex flows. The grid resolution requirement in the wall-normal direction is high and lower in the direction parallel to the wall. Despite a few issues at the RANS-LES interface regarding the compatibility of the turbulence condition, this approach is considered competent in simulating several complex flow problems in the cited studies [165–170].

Furthermore, DES recovers sub-grid models in the turbulent region and respective RANS models in the near-wall region [171]. In recent years, several studies have employed DES to study the quality of wind flow simulation over blocks (buildings). In general, the accuracy of DES is reported to be almost at the LES level by consuming lower computational resources [172, 173]. Delayed detached eddy simulation (DDES) and improved delayed detached eddy simulation (IDDES) are two recently designed modifications of the DES model. The primary alteration is done to the dissipation rate term of the turbulent kinetic energy transport equation; consequently, the turbulent length scale expressions are adjusted in the modified formulations [171]. Flow around a 6 m cube was simulated by employing IDDES in the study [171]; subsequently, the surface pressure coefficients were compared with full-scale measurements and LES results. The cited study reveals that the IDDES model captures the mean surface pressures on the windward, leeward, and lateral sides, but not on the roof of the cubic building. Moreover, the maximum, minimum, and standard deviation of surface pressure coefficients from IDDES are comparable to those obtained from LES. Moreover, the literature reveals that LES and DDES exhibit superior performance in the wake and on the lateral sides when compared to wind tunnel results [174]. Additionally, it is observed that DDES moderately recreates mean and instantaneous flow fields, very similar to pure LES ($R = 0.90$), with approximately 20% reduction in mesh number and computation time. Furthermore, the mean flow field from DDES is comparable to experimental results [175]. However, like LES, the DES models are responsive to numerical and

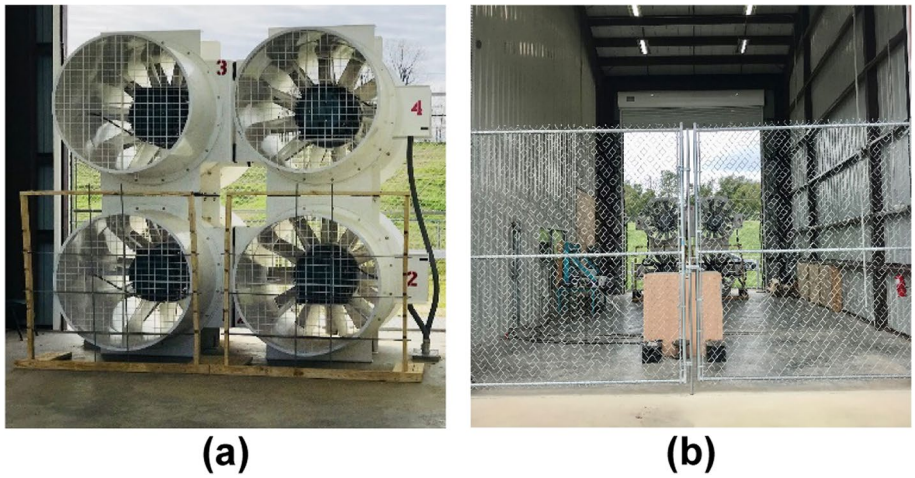

Fig. 6 LSU WISE Open-jet: (**a**) Open-jet with flow management frame, and (**b**) Instrumented cube

physical parameters [176]. Additionally, Fig. 5 compares the ability of previously conducted hybrid RANS-LES (DES) simulations to produce peak pressures with regards to full-scale data. Such simulation cases show promising results in reproducing peak pressures on the vertical ring. However, differences are noticed on the roof and the leeward face of the cube. The opportunity for improvement is evident with the hybrid cases as well. Furthermore, the dynamic hybrid RANS-LES, alternately known as dynamic linear unified RANS-LES model (DLUM), offers a superior performance of simulating turbulent flow at high Reynolds numbers; besides, DLUM allows a significant reduction in computational cost compared to LES. Moreover, the hybrid method is more accurate than the RANS and under-resolved LES simulations [177]. Furthermore, the two-layer model (TLM) or zonal model, presented in Ref. [178], is also capable of addressing similar flow problems.

6 Large-scale testing

A brief discussion on large-scale aerodynamic testing and a case study, employing open-jet testing, will be covered in this section. Large-scale experiments are appreciated since the performances of wind tunnel experiments are indecisive as a validation tool for CFD solutions. The purpose of the case study in this paper is to demonstrate the ability to conduct aerodynamic testing at higher Reynolds numbers and large scale; additionally, these capabilities add to the uniqueness of the WISE research group at LSU.

6.1 Aerodynamic testing at LSU open-jet

As part of developing aerodynamic testing capabilities, small and large open-jet facilities were built at the Windstorm Impact, Science and Engineering (WISE) research lab, Louisiana State University (LSU). Unlike wind tunnels, in open-jet testing, the flow has no physical boundaries. This means that larger eddies can be reproduced, leading to higher peak pressures, like those in the field, under minimum blockage constraints [33]. To enable the testing of larger model scales at higher Reynolds numbers, a powerful open-jet

Table 5 Model information

test facility	geometric scale (w.r.t. the 16 m cube)	geometric scale (w.r.t. the 6 m Silsoe cube)	cube-height (m)
TPU wind tunnel	1:100	1:38	0.16
LSU open-jet	1:13	1:5	1.22

facility is now operational at LSU (Fig. 6). Table 5 presents the comparison of model information used in the LSU open-jet and the TPU wind tunnel.

In this study, a fully instrumented wooden cube is tested in the open-jet facility to determine surface pressures on the cube. The wooden cube is built followed by instrumenting with pressure measuring tubes, connectors, and scanners. A metal rod is welded to a metal base to record the velocities at different heights using two cobra probes. From the collected data, plots for mean velocity and turbulence intensity profiles are made. The vertical profiles are compared with those from the TPU wind tunnel. The idea is to make meaningful comparison by running experiments under similar flow profiles.

The LSU open jet has four blowers with independent control units outside the jet chamber. The four blowers can be operated at different angular speeds to produce flow of different terrain categories; besides, there is an adjustable flow management device in front of the two lower blowers to reach target ABL flow profiles. The flow management frame was adjusted to achieve flow features on open-terrain category ($z_0 = 0.01 \sim 0.03$) [80]. The target vertical profiles are presented as a reference in Fig. 7. There is a range of target profiles that can be generated depending on the roughness length's value. However, Fig. 7 indicates that the experimental profiles represent open-terrain flow characteristics. The comparison of the along wind turbulence intensity profiles from experimental data is presented in Fig. 7 (b); the corresponding equations for Engineering Sciences Data Unit (ESDU) formulations are obtained from [179]. LSU open-jet can generate 20% turbulence intensity at reference height. Both the vertical profiles in Fig. 7 show that LSU open-jet facility can replicate ABL representing a terrain type similar to the wind tunnel. Figure 8 presents the normalized velocity spectrum corresponding to velocity measured in the jet facility. The Von-Karman formulation for normalized velocity spectra is obtained from [180]. In Fig. 8, the power spectral density, $S\ [m^2 s^{-1}]$, is normalized by multiplying with $\frac{n}{(U_{ref})^2}$ on the y-axis and, the frequency, $n\ [Hz]$, is normalized by multiplying with $\frac{z}{U_{ref}}$ on the x-axis. Here, $z\ [m]$ is the roof height of the building and $U_{ref}\ [ms^{-1}]$ is the mean velocity (reference) at that height. Besides, the von Karman theoretical spectrum is generated by using a slightly modified formulation to remain consistent with the normalizing factor. Fig. 8 reveals the energy content of the small- and large-scale eddies in the flow; the open jet flow appears to agree well with the theoretical energy content over the entire frequency range. The open-jet demonstrates producing larger turbulent eddies as the low-frequency part has a better match with the corresponding end of the theoretical spectra. Additionally, it has an acceptable energy level of small eddies in the incident flow at the building location. Therefore, the open-jet improves the overall turbulence content of the flow, when compared to small-scale wind

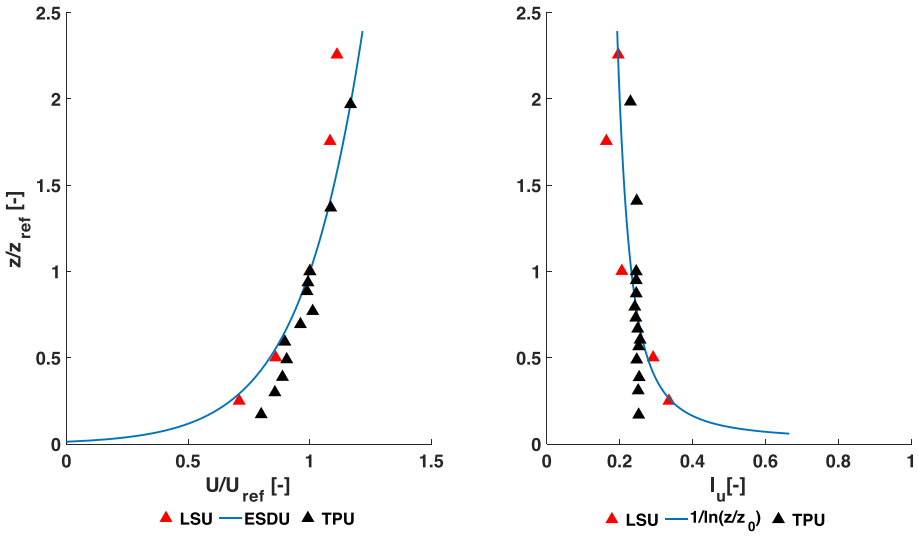

Fig. 7 Along-wind velocity measurements in the open-jet facility at 1.5H (**a**) mean-velocity profiles, and (**b**) turbulence intensity profiles

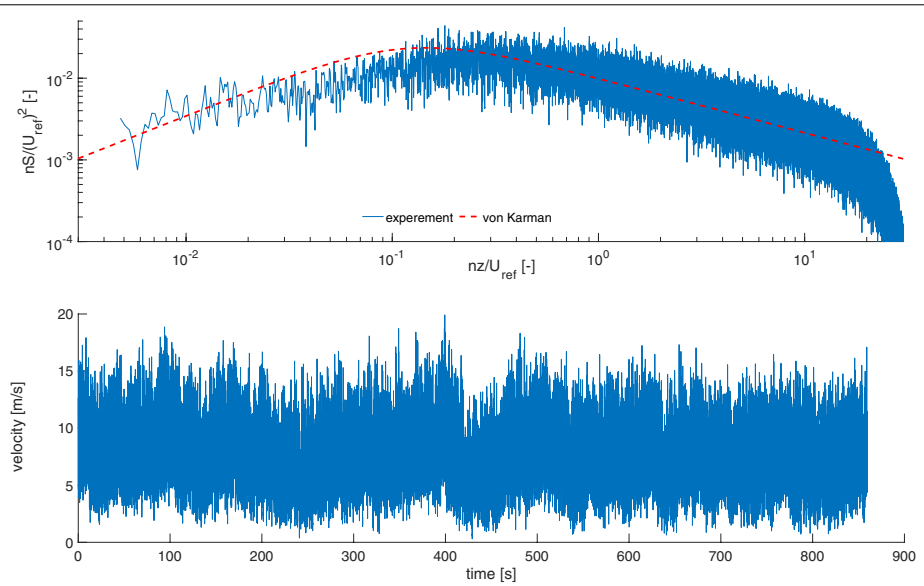

Fig. 8 Velocity spectrum and time history

tunnels that have missing low-frequency fluctuations. However, Fig. 9 demonstrates that the turbulence content is not regulated merely by varying the velocities in the same test section, and at the same elevation and position in the test facility. The integral length scale of turbulence is governed by the scale of the model, size of the test section, and the location of model in the jet facility as well. The integral length scale is expected to be greater in size than the large-scale models being tested for accurate wind load predictions [24]. Velocities were recorded at mean velocities ~8 m/s (low-speed case) and ~11 m/s (high-speed case, referred as HS in Fig. 9) at location 1.5 H and 2 H, where H is the height of test section. It is noticed that the energy content in the low and high

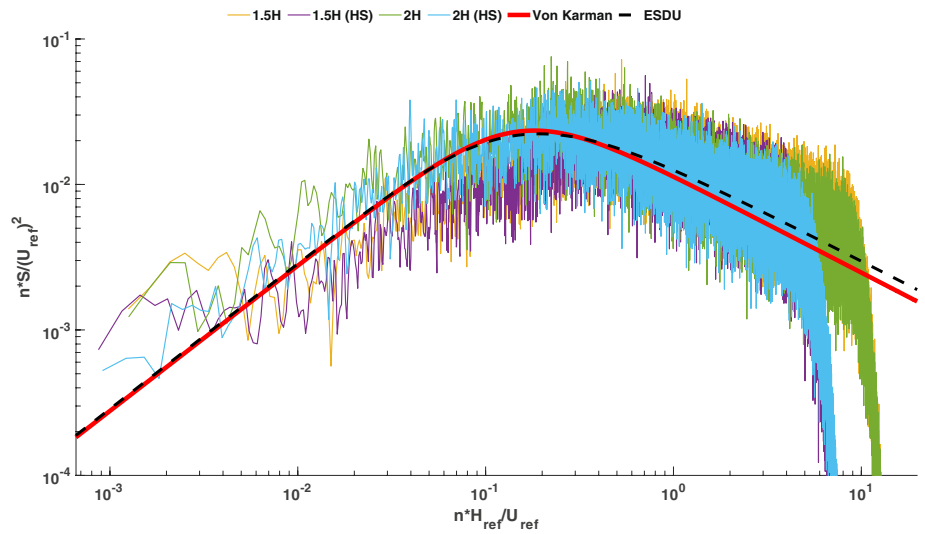

Fig. 9 Comparison of turbulence content by varying velocities

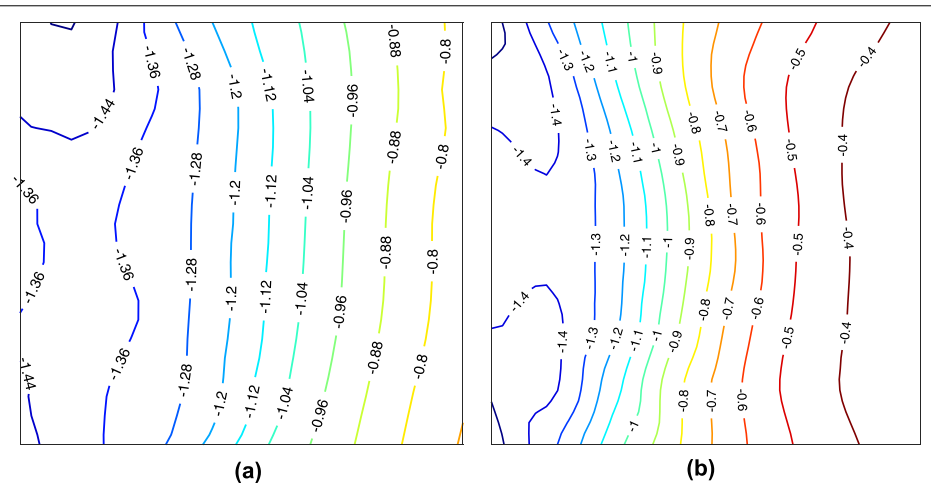

Fig. 10 Mean pressure coefficients (0 deg.): (**a**) LSU open-jet, and (**b**) TPU wind tunnel (wind from left to right)

frequencies of the turbulence spectra are comparable to the target spectra. This shows that by mere adjustment of velocities practical significance *Re effects* may not be realized. *Re effects* need to be investigated at different velocities with adequately large model and test section. In the LSU open jet Reynolds number (R_e~10^6) comparable to full-scale flow scenarios can be reproduced, whereas, in most small-scale experiments, operation at full capacity may produce R_e~10^4. Therefore, to capture true real-world flow physics solely varying velocities may not produce desirable outcomes.

The pressure-time history is recorded, and the contour of pressure coefficients is presented for the roof of the cubic building model for the 0-degree case (Figs. 10 and 11). Sixty four pressure taps are placed on the roof of the large-scale cubic model to make

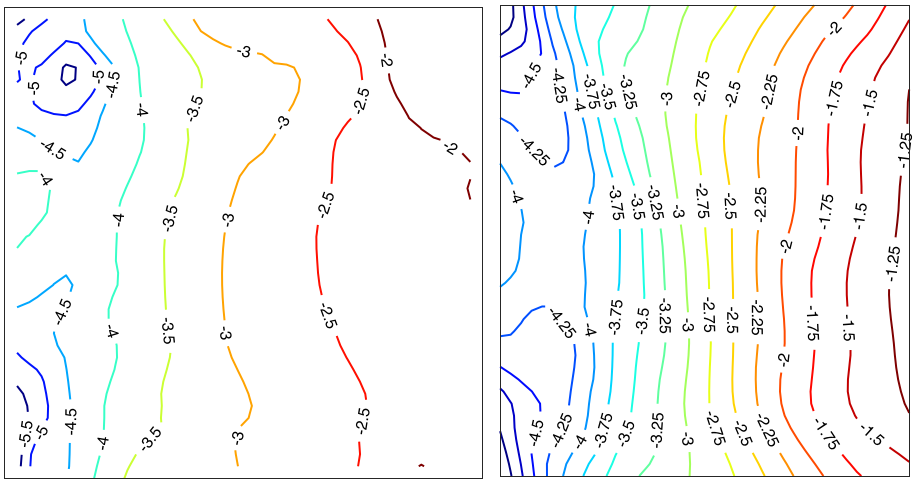

Fig. 11 Pressure coefficients' minimum (peak) values (0 deg.): (**a**) LSU open-jet, and (**b**) TPU wind tunnel (wind from left to right)

a fair comparison with results from the TPU wind tunnel. The experimental strategy involved recording and processing the time history of pressure and velocity data. Each pressure tap is connected to the Scanivalve pressure scanner via appropriate tubing. High-resolution velocity recording devices, Cobra probes, are employed to capture small changes in wind velocity. For monitoring pressure and velocity, the aforementioned instruments are installed and employed in a way that is followed in the study [66]. The sampling frequencies pressure and velocity readings were 625 Hz and 1250 Hz, respectively. The following equation is used to compute the pressure coefficient.

$$C_p(t) = \frac{p(t) - p_s}{\left(\frac{1}{2}\right)\rho U^2} \tag{1}$$

Here, ρ is the air density and U is the mean velocity at roof height. The time history of pressure coefficient, $C_p(t)$ is obtained from pressure-time history, $p(t)$ recorded using pressure scanners. The pressure is recorded before and after running the fans of the open-jet to assess the static pressure. Later, the mean value of the before and after readings (p_s) is subtracted from the pressure-time history. The above equation accounts for the differences in reference pressures for proper comparison. Once the time history of the pressure coefficient is calculated, statistical analysis is conducted to obtain the mean and minimum values of the pressure coefficients on the roof.

6.2 Experimental results and discussion

A comparison of pressure coefficients from open-jet testing at LSU with those collected from the TPU wind tunnel database is conducted. Maximum and minimum pressures are obtained utilizing a MATLAB function implementing a probabilistic approach [181]. This approach is considered because of the variability in observed peaks from one

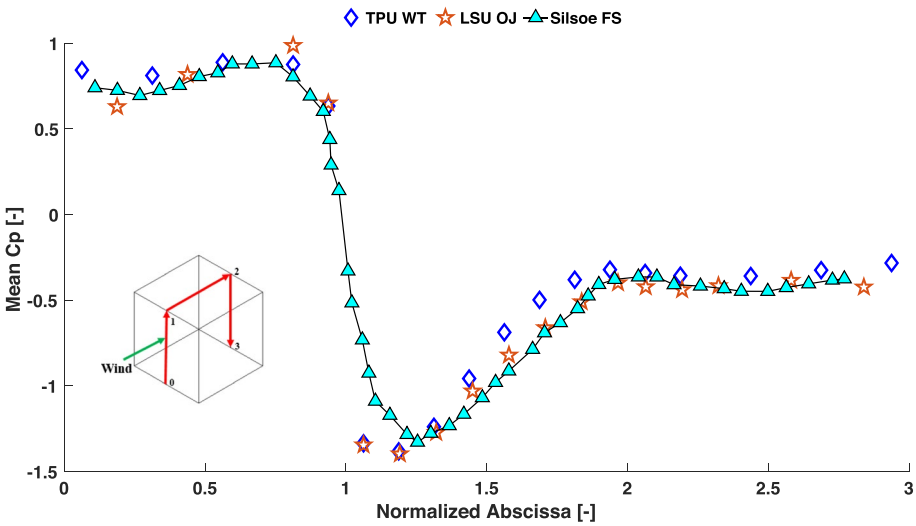

Fig. 12 Comparison of mean pressure coefficients along the vertical ring of the cube

realization to another, which stems from the highly fluctuating nature of wind. In the experiment, the angle of incidence is normal to the windward face of the cube, which is considered as the 0-degree case in this paper.

The contour plots of pressure coefficients reveal results with expected differences. The distribution of pressure coefficients is symmetric, and an identical pattern is noticed from the tunnel. The area-averaged mean and peak pressure coefficients from the TPU wind tunnel are -0.839 and -2.865 respectively; whereas the same obtained and processed from the LSU open jet facility are -0.915 and -3.267 respectively (Figs. 10 and 11). Hence, there is about 9% and 14% increase in mean and peak pressure coefficients (area-averaged) respectively, when the LSU open jet facility is employed. The open-jet test reveals higher negative pressure on the roof of the cube compared to the TPU wind tunnel. A higher suction force in open-jet testing is found due to higher Reynolds numbers and the presence of large eddies, resulting from large test section and model, relative to the situation in a wind tunnel. These disparities between the large-scale open-jet facilities and small-scale wind tunnels lead to differences in the following parameters: (a) location and size of the separation bubble, (b) stagnation point on the frontal face, and (c) length of reattachment. Likewise, differences between full-scale and small-scale wind tunnel experiments exist because of identical reasons. Near the roof corners, an increase in peak pressure coefficients is observed in the LSU open-jet compared to the TPU wind tunnel. Although the numerical values of mean pressure coefficients from both sources (Fig. 10) are in a close range (~1), the rise in pressure coefficients from open jet prediction is compelling. This increase (about 9% for mean and about 14% for peak values) can be crucial for improving buildings' resilience in powerful winds. Figure 12 reflects on the mean pressure coefficients' distributions along the vertical ring of the cube obtained from the TPU wind tunnel, LSU open jet, and the Silsoe full-scale measurements. Careful observation of the frontal face assists to realize that the mean pressure coefficients are consistent in relation to reference pressures; therefore, the observed differences on the roof are not because of the variations in reference pressures. Furthermore, the

results from large-scale open jet are encouraging in the pursuit replicating true flow physics at full-scale, which can be influential in augmenting the design standards. Since it has been mentioned earlier that the design standards underestimate design wind loads primarily because of its dependence on small-scale (such as 1:100 in TPU wind tunnel) experiments. Our upcoming paper will compare the results with pressures from a full-scale building.

7 Conclusion

This review article identifies the limitations of the prevailing ABL simulation techniques and introduces some promising experimental and computational approaches to address existing challenges. The concluding remarks are divided into the following two portions.

7.1 Part I: from literature review

- The assumptions of Reynolds number independence are questionable from the review of old and recent studies on this topic. Prediction of peak aerodynamic loads due to Reynolds number mismatch is a leading problem prevailing in wind engineering of low-rise buildings. In real ABL flow $R_e = 10^7$ (approximately) is observed, whereas, in the common wind tunnel and CFD analysis $R_e = 10^4$ is encountered.
- The improper simulation of turbulence characteristics, modeling errors of structural details, and dissimilarity in Reynolds and Jensen numbers are considered decisive factors responsible for the identified shortcomings of SSL experiments. The incompetence of such (such as, small wind tunnels) experiments to produce both small and large-scale turbulent eddies leads to inaccurate peak pressure estimations, which contributes to the inconsistencies observed in the ASCE standards.
- This paper points out the discrepancies in the recent versions of ASCE standards despite the gradual improvement in surface pressures' provisions. The design wind loads stipulated in ASCE 7–16 are conservative and uneconomical when compared to small-scale wind tunnel experiments, whereas, the same guidelines prove to be inadequate when compared with large-scale open jet testing.
- Besides documenting some promising results in building aerodynamics, the study identified a number of challenging issues with LES. LES can be more powerful and affordable if the following issues are addressed in future research endeavors.

  - Improving energy content of under-resolved or unresolved eddies in the flow.
  - Reproducing both small and large eddies over the entire frequency range by consuming affordable computational resources.
  - Establishing best practice guidelines.
  - Conducting more sensitivity analysis.
  - Validation of LES results using full-scale measurements or large-scale testing.
  - Augmenting performance of LES for flow over complex geometries and at higher Reynolds numbers.
  - Prediction of mean values on the downstream portion of roofs of sharped-edged buildings.
  - Accurate estimation of peak pressures.

  - Reducing the computational expense of LES applications at high Reynolds numbers.

- Despite some notable promising results, this paper identifies several inconsistencies concerning pressure coefficients, especially, peak values, using CFD. Moreover, the necessity of validating LES results with respect to full-scale measurements or large-scale testing is conferred. To address this issue, conducting transient CFD simulations at high Reynolds numbers is recommended.
- CFD simulations at high Reynolds numbers pose overwhelming computational challenges. The application of WMLES and hybrid RANS-LES models such as DES, DDES, IDDES, and DLUM are suggested in future studies to overcome these challenges. Also, assessing the performance of different SGS models with LES is highly encouraged to reduce computational costs.

7.2 Part II: from the case study

- The case study reveals that the mean and peak pressure coefficients are higher for the large-scale model (compared to the small-scale wind tunnel results). The open-jet results are comparable to full-scale measurements.
- These differences are due to extensive flow separation and longer reattachment length along the roof in case of large-scale testing in open-jet; additionally, the higher Reynolds number and presence of large eddies in large-scale open-jet testing contributed to higher surface pressure measurements.
- The experimental results strengthen our hypothesis about the scaling issue and the Reynolds number effect. Investigating R_e *effects* merely by adjusting velocities in a small-scale laboratory will not produce desirable and precise pressure predictions. Experimentally, larger test sections are necessary to ensure growth and development of large eddies that result in accurate peak pressures.
- The results are encouraging and will facilitate future research in building aerodynamics. The conducted experiment is a groundwork for future studies to address the limitations highlighted in the review part.

Acknowledgements
Several students at the WISE Lab helped with the building of the aerodynamic test model.

Authors' contributions
The two authors contributed equally to the planning, aerodynamic testing, data analysis, and the writing of the paper. The authors read and approved the final manuscript.

Funding
The second author (A.M. Aly) received financial support from the Louisiana Board of Regents (RCS, LEQSF(2021–22)-RD-A-30). Also, the second author received funds from the NSF I-Corps program at Louisiana State University. The findings are those of the authors and do not necessarily reflect the position of the funding sponsors.

Availability of data and materials
The datasets generated during the current study are available from the corresponding author on reasonable request.

Declarations

Competing interests
The authors declare that they have no competing interests.

Received: 9 January 2022 Accepted: 6 April 2022
Published online: 01 June 2022

References

1. Uematsu Y, Isyumov N (1999) Wind pressures acting on low-rise buildings. J Wind Eng Ind Aerodyn 82:1–25. https://doi.org/10.1016/S0167-6105(99)00036-7
2. Pindado S, Meseguer J (2003) Wind tunnel study on the influence of different parapets on the roof pressure distribution of low-rise buildings. J Wind Eng Ind Aerodyn 91:1133–1139. https://doi.org/10.1016/S0167-6105(03)00055-2
3. Holmes JD, Syme MJ, Kasperski M (1995) Optimised design of a low-rise industrial building for wind loads. J Wind Eng Ind Aerodyn 57:391–401. https://doi.org/10.1016/0167-6105(94)00105-M
4. Wang T, Cao S, Ge Y (2014) Effects of inflow turbulence and slope on turbulent boundary layer over two-dimensional hills. Wind Struct 19:219–232
5. Zhou Q, Cao S, Zhou Z (2013) Numerical studies on non-shear and shear flows past a 5:1 rectangular cylinder. Wind Struct 17:379–397
6. Simiu E (2011) Design of Buildings for wind: a guide for ASCE 7–10 standard users and designers of special structures, 2nd edn. Wiley, Hoboken. https://doi.org/10.1002/9781118086131
7. Aly AM (2014) Atmospheric boundary-layer simulation for the built environment: past, present and future. Build Environ 75:206–221. https://doi.org/10.1016/j.buildenv.2014.02.004
8. Wang D, Yu XJ, Zhou Y, Tse KT (2015) A combination method to generate fluctuating boundary conditions for large eddy simulation. Wind Struct 20:579–607
9. Chan CM, Ding F, Tse KT, Huang MF, Shum KM, Kwok KCS (2019) Optimal wind-induced load combinations for structural design of tall buildings. Wind Struct 29:323–337
10. Keerthana M, Harikrishna P (2017) Wind tunnel investigations on aerodynamics of a 2:1 rectangular section for various angles of wind incidence. Wind Struct 25:301–328
11. Zhang J, Zhang M, Li Y, Fang C (2019) Aerodynamic effects of subgrade-tunnel transition on high-speed railway by wind tunnel tests. Wind Struct 28:203–213
12. Ghazal T, Chen J, Aboutabikh M, Aboshosha H, Elgamal S (2020) Flow-conditioning of a subsonic wind tunnel to model boundary layer flows. Wind Struct 30:339–366
13. Zhang M, Zhang J, Li Y, Yu J, Zhang J, Wu L (2020) Wind characteristics in the high-altitude difference at bridge site by wind tunnel tests. Wind Struct 30:547–558
14. Jafari M, Sarkar PP (2020) Wind tunnel study of wake-induced aerodynamics of parallel stay-cables and power conductor cables in a yawed flow. Wind Struct 30:617–631
15. Ryu H-J, Shin D-H, Ha Y-C (2020) Serviceability evaluation methods for high-rise structures considering wind direction. Wind Struct 30:275–288
16. Elshaer A, Bitsuamlak G, Abdallah H (2019) Variation in wind load and flow of a low-rise building during progressive damage scenario. Wind Struct 28:389–404
17. Ibrahim I, Aboshosha H, El Damatty A (2020) Numerical characterization of downburst wind field at WindEEE dome. Wind Struct 30:231–243
18. Lee M, Lee SH, Hur N, Choi C-K (2010) A numerical simulation of flow field in a wind farm on complex terrain. Wind Struct 13:375
19. Lancelot PMGJ, Sodja J, Werter NPM, De Breuker R (2017) Design and testing of a low subsonic wind tunnel gust generator. Adv Aircr Spacecr Sci 4:125
20. Yang MY, Palodichuk MT (2019) Recommendations on dynamic pressure sensor placement for transonic wind tunnel tests. Adv Aircr Spacecr Sci 6:497–513
21. Cheng XX, Zhao L, Ge YJ, Dong J, Demartino C (2017) A comprehensive high Reynolds number effects simulation method for wind pressures on cooling tower models. Wind Struct 24:119–144
22. Su Y, Xiang H, Fang C, Wang L, Li Y (2017) Wind tunnel tests on flow fields of full-scale railway wind barriers. Wind Struct 24:171–184
23. Wang XJ, Li QS, Yan BW (2020) Full-scale measurements of wind pressures on a low-rise building during typhoons and comparison with wind tunnel test results and aerodynamic database. J Struct Eng 146. https://doi.org/10.1061/(asce)st.1943-541x.0002769
24. Mooneghi MA, Irwin P, Chowdhury AG (2016) Partial turbulence simulation method for predicting peak wind loads on small structures and building appurtenances. J Wind Eng Ind Aerodyn 157:47–62. https://doi.org/10.1016/j.jweia.2016.08.003
25. Stenabaugh SE, Iida Y, Kopp GA, Karava P (2015) Wind loads on photovoltaic arrays mounted parallel to sloped roofs on low-rise buildings. J Wind Eng Ind Aerodyn 139:16–26. https://doi.org/10.1016/j.jweia.2015.01.007
26. Karimpour A, Kaye NB (2013) Wind tunnel measurement of the parapet height role on roof gravel blow-off rate for two dimensional low rise buildings. J Wind Eng Ind Aerodyn 114:38–47. https://doi.org/10.1016/j.jweia.2012.12.007
27. Fritz WP, Bienkiewicz B, Cui B et al (2008) International comparison of wind tunnel estimates of wind effects on low-rise buildings: test-related uncertainties. J Struct Eng 134:1887–1890. https://doi.org/10.1061/(ASCE)0733-9445(2008)134:12(1887)

28. Kargarmoakhar R, Chowdhury AG, Irwin PA (2015) Reynolds number effects on twin box girder long span bridge aerodynamics. Wind Struct 20:327–347. https://doi.org/10.12989/was.2015.20.2.327
29. Simiu E, Letchford C, Isyumov N, Chowdhury AG, Yeo D (2013) Assessment of ASCE 7-10 standard methods for determining wind loads. J Struct Eng 139:2044–2047. https://doi.org/10.1061/(ASCE)ST.1943-541X.0000771
30. Zisis I, Stathopoulos T (2009) Wind-induced cladding and structural loads on low-wood building. J Struct Eng 135:437–447. https://doi.org/10.1061/(Asce)0733-9445(2009)135:4(437)
31. Huang S, Li QS, Xu S (2007) Numerical evaluation of wind effects on a tall steel building by CFD. J Constr Steel Res 63:612–627. https://doi.org/10.1016/j.jcsr.2006.06.033
32. Ong RH, Patruno L, Yeo D, He Y, Kwok KCS (2020) Numerical simulation of wind-induced mean and peak pressures around a low-rise structure. Eng Struct 214:110583. https://doi.org/10.1016/j.engstruct.2020.110583
33. Aly AM, Khaled F, Gol-Zaroudi H (2020) Aerodynamics of low-rise buildings: challenges and recent advances in experimental and computational methods. In Gorji-Bandpy M, Aly A (eds) Aerodynamics. IntechOpen. https://doi.org/10.5772/intechopen.92794
34. Lim HC, Castro IP, Hoxey RP (2007) Bluff bodies in deep turbulent boundary layers: Reynolds-number issues. J Fluid Mech 571:97–118. https://doi.org/10.1017/S0022112006003223
35. Cherry NJ, Hillier R, Latour MEM (1984) Unsteady measurements in a separating and reattaching flow. J Fluid Mech 144:13–46
36. Djilali N, Gartshore IS (1991) Turbulent flow around a bluff rectangular plate. Part I: experimental investigation. J Fluids Eng 113:51–59
37. Sohankar A (2006) Flow over a bluff body from moderate to high Reynolds numbers using large eddy simulation. Comput Fluids 35:1154–1168. https://doi.org/10.1016/j.compfluid.2005.05.007
38. Hoxey RP, Reynolds AM, Richardson GM, Robertson AP, Short JL (1998) Observations of Reynolds number sensitivity in the separated flow region on a bluff body. J Wind Eng Ind Aerodyn 73:231–249. https://doi.org/10.1016/S0167-6105(97)00287-0
39. Driss S, Driss Z, Kammoun IK (2014) Study of the Reynolds number effect on the aerodynamic structure around an obstacle with inclined roof. Sustain Energy 2:126–133. https://doi.org/10.1007/978-3-319-14532-7_14
40. Wang B, Wang Z, Cui G, Zhang Z (2014) Study on the dynamic characteristics of flow over building cluster at high Reynolds number by large eddy simulation. Sci China Phys Mech Astron 57:1144–1159. https://doi.org/10.1007/s11433-014-5453-x
41. Ding F, Kareem A, Wan J (2019) Aerodynamic tailoring of structures using computational fluid dynamics. Struct Eng Int 29:26–39. https://doi.org/10.1080/10168664.2018.1522936
42. Tieleman HW (2003) Wind tunnel simulation of wind loading on low-rise structures: a review. J Wind Eng Ind Aerodyn 91:1627–1649. https://doi.org/10.1016/j.jweia.2003.09.021
43. Levitan ML, Mehta KC (1992) Texas Tech field experiments for wind loads part 1: building and pressure measuring system. J Wind Eng Ind Aerodyn 43:1565–1576. https://doi.org/10.1016/0167-6105(92)90372-H
44. Sill BL, Cook NJ, Fang C (1992) The Aylesbury comparative experiment: a final report. J Wind Eng Ind Aerodyn 43:1553–1564. https://doi.org/10.1016/0167-6105(92)90371-G
45. Richards PJ, Hoxey RP, Short LJ (2001) Wind pressures on a 6 m cube. J Wind Eng Ind Aerodyn 89:1553–1564. https://doi.org/10.1016/S0167-6105(01)00139-8
46. Apperley L, Surry D, Stathopoulos T, Davenport AG (1979) Comparative measurements of wind pressure on a model of the full-scale experimental house at Aylesbury, England. J Wind Eng Ind Aerodyn 4:207–228. https://doi.org/10.1016/0167-6105(79)90002-3
47. Hoxey RP, Richards PJ (1993) Flow patterns and pressure field around a full-scale building. J Wind Eng Ind Aerodyn 50:203–212. https://doi.org/10.1016/0167-6105(93)90075-Y
48. Doudak G, McClure G, Smith I, Hu L, Stathopoulos T (2005) Monitoring structural response of a wooden light-frame industrial shed building to environmental loads. J Struct Eng 131:794–805. https://doi.org/10.1061/(ASCE)0733-9445(2005)131:5(794)
49. Caracoglia L, Jones NP (2009) Analysis of full-scale wind and pressure measurements on a low-rise building. J Wind Eng Ind Aerodyn 97:157–173. https://doi.org/10.1016/j.jweia.2009.06.001
50. Lim HC, Thomas TG, Castro IP (2009) Flow around a cube in a turbulent boundary layer: LES and experiment. J Wind Eng Ind Aerodyn 97:96–109. https://doi.org/10.1016/j.jweia.2009.01.001
51. Aly AM, Chowdhury AG, Bitsuamlak G (2011) Wind profile management and blockage assessment for a new 12-fan wall of wind facility at FIU. Wind Struct 14:285–300. https://doi.org/10.12989/was.2011.14.4.285
52. Guichard R (2019) Assessment of an improved random flow generation method to predict unsteady wind pressures on an isolated building using large-eddy simulation. J Wind Eng Ind Aerodyn 189:304–313. https://doi.org/10.1016/j.jweia.2019.04.006
53. Tokyo Polytechnic University (2007) Aerodynamic database for low-rise buildings http://wind.arch.t-kougei.ac.jp/system/eng/contents/code/tpu
54. Murakami S, Mochida A, Hayashi Y (1990) Examining the κ-ϵ model by means of a wind tunnel test and large-eddy simulation of the turbulence structure around a cube. J Wind Eng Ind Aerodyn 35:87–100. https://doi.org/10.1016/0167-6105(90)90211-T
55. Tieleman HW (1996) Model/full scale comparison of pressures on the roof of the TTU experimental building. J Wind Eng Ind Aerodyn 65:133–142. https://doi.org/10.1016/S0167-6105(97)00030-5
56. Hagos A, Habte F, Chowdhury AG, Yeo D (2014) Comparisons of two wind tunnel pressure databases and partial validation against full-scale measurements. J Struct Eng 140. https://doi.org/10.1061/(ASCE)ST.1943-541X.0001001
57. Long F (2004) Uncertainties in pressure coefficients derived from full and model scale data. Dissertation, Texas Tech University https://ttu-ir.tdl.org/handle/2346/15683?locale-attribute=de
58. Xu YL (1995) Model- and full-scale comparison of fatigue-related characteristics of wind pressures on the Texas Tech building. J Wind Eng Ind Aerodyn 58:147–173. https://doi.org/10.1016/0167-6105(95)00012-7
59. Cheung JCK, Holmes JD, Melbourne WH, Lakshmanan N, Bowditch P (1997) Pressures on a 1/10 scale model of the Texas Tech building. J Wind Eng Ind Aerodyn 69–71:529–538

60. Zisis I, Stathopoulos T (2012) Wind load transfer mechanisms on a low wood building using full-scale load data. J Wind Eng Ind Aerodyn 104–106:65–75. https://doi.org/10.1016/j.jweia.2012.04.003
61. Li QS, Hu SY (2014) Monitoring of wind effects on a low-rise building during typhoon landfalls and comparison to wind tunnel test results. Struct Control Health Monit 21:1360–1386. https://doi.org/10.1002/stc
62. Wang X, Li Q, Li J (2020) Field monitoring and wind tunnel study of wind effects on roof overhang of a low-rise building. Struct Control Health Monit 27. https://doi.org/10.1002/stc.2484
63. Dalgliesh WA, Surry D (2003) BLWT, CFD and HAM modelling vs. the real world: bridging the gaps with full-scale measurements. J Wind Eng Ind Aerodyn 91:1651–1669. https://doi.org/10.1016/j.jweia.2003.09.015
64. Kopp GA, Morrison MJ, Henderson DJ (2012) Full-scale testing of low-rise, residential buildings with realistic wind loads. J Wind Eng Ind Aerodyn 104–106:25–39. https://doi.org/10.1016/j.jweia.2012.01.004
65. Huang P, Wang X, Gu M (2012) Field experiments for wind loads on a low-rise building with adjustable pitch. Int J Distrib Sens Networks 8:451879. https://doi.org/10.1155/2012/451879
66. Gol Zaroudi H, Aly AM (2017) Open-jet boundary-layer processes for aerodynamic testing of low-rise buildings. Wind Struct 25:233–259. https://doi.org/10.12989/was.2017.25.3.233
67. Jafari A, Ghanadi F, Emes MJ, Arjomandi M, Cazzolato BS (2019) Measurement of unsteady wind loads in a wind tunnel: scaling of turbulence spectra. J Wind Eng Ind Aerodyn 193:103955. https://doi.org/10.1016/j.jweia.2019.103955
68. Akins RE, Peterka JA, Cermak JE (1977) Mean force and moment coefficients for buildings in turbulent boundary layers. J Wind Eng Ind Aerodyn 2:195–209. https://doi.org/10.1016/0167-6105(77)90022-8
69. Stathopoulos T (2003) Wind loads on low buildings: in the wake of Alan Davenport's contributions. J Wind Eng Ind Aerodyn 91:1565–1585. https://doi.org/10.1016/j.jweia.2003.09.019
70. Holmes JD (2014) Along- and cross-wind response of a generic tall building: comparison of wind-tunnel data with codes and standards. J Wind Eng Ind Aerodyn 132:136–141. https://doi.org/10.1016/j.jweia.2014.06.022
71. Ho TCE, Surry D, Morrish D, Kopp GA (2005) The UWO contribution to the NIST aerodynamic database for wind loads on low buildings: part 1. Archiving format and basic aerodynamic data. J Wind Eng Ind Aerodyn 93:1–30. https://doi.org/10.1016/j.jweia.2004.07.006
72. Chen X, Zhou N (2007) Equivalent static wind loads on low-rise buildings based on full-scale pressure measurements. Eng Struct 29:2563–2575. https://doi.org/10.1016/j.engstruct.2007.01.007
73. Li QS, Hu SY, Dai YM, He YC (2012) Field measurements of extreme pressures on a flat roof of a low-rise building during typhoons. J Wind Eng Ind Aerodyn 111:14–29. https://doi.org/10.1016/j.jweia.2012.08.003
74. Gierson ML, Phillips BM, Duthinh D (2015) Evaluation of ASCE 7-10 wind velocity pressure coefficients on the components and cladding of low-rise buildings using recent wind tunnel testing data. Paper presented at the 6th International Conference on Advances in Experimental structural Engineering, Urbana, 1-2 August 2015
75. Aly AM, Gol-Zaroudi H (2020) Peak pressures on low rise buildings: CFD with les versus full scale and wind tunnel measurements. Wind Struct An Int J 30:99–117. https://doi.org/10.12989/was.2020.30.1.099
76. Kopp GA, Morrison MJ (2018) Component and cladding wind loads for low-slope roofs on low-rise buildings. J Struct Eng 144. https://doi.org/10.1061/(asce)st.1943-541x.0001989
77. Scott DR (2018) ASCE 7-16 wind load provisions. Structure Magazine: Codes and standards. p 12–14. https://www.structuremag.org/?p=13360
78. Wang J, Kopp GA (2021) Comparisons of aerodynamic data with the main wind force–resisting system provisions of ASCE 7–16. I: low-rise buildings. J Struct Eng 147. https://doi.org/10.1061/(asce)st.1943-541x.0002925
79. Aldoum M, Stathopoulos T (2020) Wind loads on low-slope roofs of buildings with large plan dimensions. Eng Struct 225:111298. https://doi.org/10.1016/j.engstruct.2020.111298
80. Aly AM, da Fonseca Yousef N (2021) High Reynolds number aerodynamic testing of a roof with parapet. Eng Struct 234:112006. https://doi.org/10.1016/j.engstruct.2021.112006
81. Rodi W (1998) Large-eddy simulations of the flow past bluff bodies: state-of-the art. JSME Int J Ser B Fluids Therm Eng 41:361–374. https://doi.org/10.1299/jsmeb.41.361
82. Shah KB, Ferziger JH (1997) A fluid mechanicians view of wind engineering: large eddy simulation of flow past a cubic obstacle. J Wind Eng Ind Aerodyn 67–68:211–224. https://doi.org/10.1016/S0167-6105(97)00074-3
83. Saeedi M, LePoudre PP, Wang BC (2014) Direct numerical simulation of turbulent wake behind a surface-mounted square cylinder. J Fluids Struct 51:20–39. https://doi.org/10.1016/j.jfluidstructs.2014.06.021
84. Bruno L, Fransos D, Coste N, Bosco A (2010) 3D flow around a rectangular cylinder: a computational study. J Wind Eng Ind Aerodyn 98:263–276. https://doi.org/10.1016/j.jweia.2009.10.005
85. Bruno L, Salvetti MV, Ricciardelli F (2014) Benchmark on the aerodynamics of a rectangular 5:1 cylinder: an overview after the first four years of activity. J Wind Eng Ind Aerodyn 126:87–106. https://doi.org/10.1016/j.jweia.2014.01.005
86. Khaled MF, Aly AM, Elshaer A (2021) Computational efficiency of CFD modeling for building engineering: an empty domain study. J Build Eng 42:102792. https://doi.org/10.1016/j.jobe.2021.102792
87. Tamura T, Nozawa K, Kondo K (2008) AIJ guide for numerical prediction of wind loads on buildings. J Wind Eng Ind Aerodyn 96:1974–1984. https://doi.org/10.1016/j.jweia.2008.02.020
88. Oberkampf WL, Trucano TG, Hirsch C (2004) Verification, validation, and predictive capability in computational engineering and physics. Appl Mech Rev. https://doi.org/10.1115/1.1767847
89. Park GI (2017) Wall-modeled large-eddy simulation of a high Reynolds number separating and reattaching flow. AIAA J 55:3709–3721. https://doi.org/10.2514/1.J055745
90. Mittal R, Moin P (1997) Suitability of upwind-biased finite difference schemes for large-eddy simulation of turbulent flows. AIAA J 35:2746–2757. https://doi.org/10.2514/2.253
91. Fröhlich J, Mellen CP, Rodi W, Temmerman L, Leschziner MA (2005) Highly resolved large-eddy simulation of separated flow in a channel with streamwise periodic constrictions. J Fluid Mech 526:19–66. https://doi.org/10.1017/S0022112004002812
92. Verma A, Mahesh K (2012) A Lagrangian subgrid-scale model with dynamic estimation of Lagrangian time scale for large eddy simulation of complex flows. Phys Fluids 24:085101. https://doi.org/10.1063/1.4737656

93. You D, Ham F, Moin P (2008) Discrete conservation principles in large-eddy simulation with application to separation control over an airfoil. Phys Fluids 20:101515. https://doi.org/10.1063/1.3006077
94. Bouffanais R (2010) Advances and challenges of applied large-eddy simulation. Comput Fluids 39:735–738. https://doi.org/10.1016/j.compfluid.2009.12.003
95. Tamura T (2008) Towards practical use of LES in wind engineering. J Wind Eng Ind Aerodyn 96:1451–1471. https://doi.org/10.1016/j.jweia.2008.02.034
96. Kawai H (2002) Local peak pressure and conical vortex on building. J Wind Eng Ind Aerodyn 90:251–263. https://doi.org/10.1016/S0167-6105(01)00218-5
97. Selvam RP (1997) Computation of pressures on Texas Tech University building using large eddy simulation. J Wind Eng Ind Aerodyn 67–68:647–657. https://doi.org/10.1016/S0167-6105(97)00107-4
98. Trias FX, Gorobets A, Oliva A (2015) Turbulent flow around a square cylinder at Reynolds number 22,000: a DNS study. Comput Fluids 123:87–98. https://doi.org/10.1016/j.compfluid.2015.09.013
99. Oberai AA, Liu J, Sondak D, Hughes TJR (2014) A residual based eddy viscosity model for the large eddy simulation of turbulent flows. Comput Methods Appl Mech Eng 282:54–70. https://doi.org/10.1016/j.cma.2014.08.014
100. Ai ZT, Mak CM (2015) Large-eddy simulation of flow and dispersion around an isolated building: analysis of influencing factors. Comput Fluids 118:89–100. https://doi.org/10.1016/j.compfluid.2015.06.006
101. Cao Y, Tamura T (2016) Large-eddy simulations of flow past a square cylinder using structured and unstructured grids. Comput Fluids 137:36–54. https://doi.org/10.1016/j.compfluid.2016.07.013
102. Cao Y, Tamura T, Kawai H (2020) Spanwise resolution requirements for the simulation of high-Reynolds-number flows past a square cylinder. Comput Fluids 196:104320. https://doi.org/10.1016/j.compfluid.2019.104320
103. Tabor GR, Baba-Ahmadi MH (2010) Inlet conditions for large eddy simulation: a review. Comput Fluids 39:553–567. https://doi.org/10.1016/j.compfluid.2009.10.007
104. Sagaut P, Deck S, Terracol M (2006) Multiscale and multiresolution approaches in turbulence. Imperial College Press, London. https://doi.org/10.1142/P447
105. Aboshosha H, Elshaer A, Bitsuamlak GT, El Damatty A (2015) Consistent inflow turbulence generator for LES evaluation of wind-induced responses for tall buildings. J Wind Eng Ind Aerodyn 142:198–216. https://doi.org/10.1016/j.jweia.2015.04.004
106. Tominaga Y, Mochida A, Yoshie R et al (2008) AIJ guidelines for practical applications of CFD to pedestrian wind environment around buildings. J Wind Eng Ind Aerodyn 96:1749–1761. https://doi.org/10.1016/j.jweia.2008.02.058
107. Xie Z-T, Castro IP (2008) Efficient generation of inflow conditions for large eddy simulation of street-scale flows. Flow Turbul Combust 81:449–470. https://doi.org/10.1007/s10494-008-9151-5
108. Keating A, Piomelli U, Balaras E, Kaltenbach H-J (2004) A priori and a posteriori tests of inflow conditions for large-eddy simulation. Phys Fluids 16:4696–4712. https://doi.org/10.1063/1.1811672
109. Liu K, Pletcher RH (2006) Inflow conditions for the large eddy simulation of turbulent boundary layers: a dynamic recycling procedure. J Comput Phys 219:1–6. https://doi.org/10.1016/j.jcp.2006.04.004
110. Lund TS, Wu X, Squires KD (1998) Generation of turbulent inflow data for spatially-developing boundary layer simulations. J Comput Phys 140:233–258. https://doi.org/10.1006/jcph.1998.5882
111. Nozawa K, Tamura T (2002) Large eddy simulation of the flow around a low-rise building immersed in a rough-wall turbulent boundary layer. J Wind Eng Ind Aerodyn 90:1151–1162. https://doi.org/10.1016/S0167-6105(02)00228-3
112. Huang SH, Li QS, Wu JR (2010) A general inflow turbulence generator for large eddy simulation. J Wind Eng Ind Aerodyn 98:600–617. https://doi.org/10.1016/j.jweia.2010.06.002
113. Kim Y, Castro IP, Xie Z-T (2013) Divergence-free turbulence inflow conditions for large-eddy simulations with incompressible flow solvers. Comput Fluids 84:56–68. https://doi.org/10.1016/j.compfluid.2013.06.001
114. Patterson JW, Balin R, Jansen KE (2020) Assessing and improving the accuracy of synthetic turbulence generation. J Fluid Mech 906. https://doi.org/10.1017/jfm.2020.859
115. Kraichnan RH (1970) Diffusion by a random velocity field. Phys Fluids 13:12–31. https://doi.org/10.1063/1.1692799
116. Karweit M, Blanc-Benon P, Juvé D, Comte-Bellot G (1991) Simulation of the propagation of an acoustic wave through a turbulent velocity field: a study of phase variance. J Acoust Soc Am 89:52–62. https://doi.org/10.1121/1.400415
117. Batten P, Goldberg U, Chakravarthy S (2004) Interfacing statistical turbulence closures with large-eddy simulation. AIAA J 42:485–482. https://doi.org/10.2514/1.3496
118. Davidson L, Billson M (2006) Hybrid LES-RANS using synthesized turbulent fluctuations for forcing in the interface region. Int J Heat Fluid Flow 27:1028–1042. https://doi.org/10.1016/j.ijheatfluidflow.2006.02.025
119. Béchara W, Bailly C, Lafon P, Candel SM (1994) Stochastic approach to noise modeling for free turbulent flows. AIAA J 32:455–463. https://doi.org/10.2514/3.12008
120. Smirnov A, Shi S, Celik I (2001) Random flow generation technique for large eddy simulations and particle-dynamics modeling. ASME J Fluids Eng 123:359–371. https://doi.org/10.1115/1.1369598
121. Shur ML, Spalart PR, Strelets MK, Travin AK (2014) Synthetic turbulence generators for RANS-LES interfaces in zonal simulations of aerodynamic and aeroacoustic problems. Flow, Turbul Combust 93:63–92. https://doi.org/10.1007/s10494-014-9534-8
122. Spalart PR, Belyaev KV, Garbaruk AV, Shur ML, Strelets MK, Travin AK (2017) Large-eddy and direct numerical simulations of the Bachalo-Johnson flow with shock-induced separation. Flow, Turbul Combust 93:865–885. https://doi.org/10.1007/s10494-017-9832-z
123. Kornev N, Hassel E (2007) Synthesis of homogeneous anisotropic divergence-free turbulent fields with prescribed second-order statistics by vortex dipoles. Phys Fluids 19:068101. https://doi.org/10.1063/1.2738607
124. Poletto R, Revell A, Craft T, Jarrin N (2011) Divergence free synthetic eddy method for embedded LES inflow boundary conditions. In: Proceedings of the 7th International Symposium on Turbulence and Shear Flow Phenomena, Ottawa
125. Poletto R, Craft T, Revell A (2013) A new divergence free synthetic eddy method for the reproduction of inlet flow conditions for LES. Flow, Turbul Combust 91:519–539. https://doi.org/10.1007/s10494-013-9488-2

126. Patruno L, Ricci M (2018) A systematic approach to the generation of synthetic turbulence using spectral methods. Comput Methods Appl Mech Eng 340:881–904. https://doi.org/10.1016/j.cma.2018.06.028
127. Kröger H, Kornev N (2018) Generation of divergence free synthetic inflow turbulence with arbitrary anisotropy. Comput Fluids. https://doi.org/10.1016/j.compfluid.2018.01.018
128. Patruno L, Ricci M (2017) On the generation of synthetic divergence-free homogeneous anisotropic turbulence. Comput Methods Appl Mech Eng 315:396–417. https://doi.org/10.1016/j.cma.2016.11.005
129. Fung JCH, Hunt JCR, Malik NA, Perkins RJ (1992) Kinematic simulation of homogeneous turbulence by unsteady random Fourier modes. J Fluid Mech 236:281–318. https://doi.org/10.1017/S0022112092001423
130. Castro G, Paz RR, Sonzogni V (2011) Generation of turbulent inlet velocity conditions for large eddy simulations. Mecánica Comput XXX:2275–2288
131. Woo KR, Bok LI, Seok KK (2017) Evaluation of wind pressure acting on multi-span greenhouses using CFD technique, part 1: development of the CFD model. Biosyst Eng 164:235–256. https://doi.org/10.1016/j.biosystemseng.2017.09.008
132. Woo KR, Bok LI, Hyeon YU, Yeon LS (2019) Estimating the wind pressure coefficient for single-span greenhouses using an large eddy simulation turbulence model. Biosyst Eng 188:114–135. https://doi.org/10.1016/j.biosystemseng.2019.10.009
133. Janajreh I, Simiu E (2012) Large eddy simulation of wind loads on a low-rise structure and comparison with wind tunnel results. Appl Mech Mater 152–154:1806–1813. https://doi.org/10.4028/www.scientific.net/AMM.152-154.1806
134. Liu Z, Yu Z, Chen X, Cao R, Zhu F (2020) An investigation on external airflow around low-rise building with various roof types: PIV measurements and LES simulations. Build Environ 169:106583. https://doi.org/10.1016/j.buildenv.2019.106583
135. Xing F, Mohotti D, Chauhan K (2018) Study on localised wind pressure development in gable roof buildings having different roof pitches with experiments, RANS and LES simulation models. Build Environ. https://doi.org/10.1016/j.buildenv.2018.07.026
136. Richards P, Norris S (2015) LES modelling of unsteady flow around the Silsoe cube. J Wind Eng Ind Aerodyn 144:70–78. https://doi.org/10.1016/j.jweia.2015.03.018
137. Nozawa K, Ohashi M, Tamura T, Okuda Y (2009) LES study on urban roughness effects on turbulence statistics of atmospheric boundary layer. Paper presented at the 5th European & African conference on wind engineering, Florence
138. Cindori M, Juretić F, Kozmar H, Džijan I (2018) Steady RANS model of the homogeneous atmospheric boundary layer. J Wind Eng Ind Aerodyn 173:289–301. https://doi.org/10.1016/j.jweia.2017.12.006
139. Köse DA, Dick E (2010) Prediction of the pressure distribution on a cubical building with implicit LES. J Wind Eng Ind Aerodyn 98:628–649. https://doi.org/10.1016/j.jweia.2010.06.004
140. Richards PJ, Hoxey RP (2012) Pressures on a cubic building—part 1: full-scale results. J Wind Eng Ind Aerodyn 102:72–86. https://doi.org/10.1016/j.jweia.2011.11.004
141. Krajnović S, Müller D, Davidson L (1999) Comparison of two one-equation subgrid models in recirculating flows. In: Voke PR, Sandham ND, Kleiser L (eds) Direct and large-eddy simulation III. ERCOFTAC Series, vol 7. Springer, Dordrecht. https://doi.org/10.1007/978-94-015-9285-7_6
142. Hertwig D, Patnaik G, Leitl B (2017) LES validation of urban flow, part I: flow statistics and frequency distributions. Environ Fluid Mech 17:521–550. https://doi.org/10.1007/s10652-016-9507-7
143. Liu J, Niu J, Du Y, Mak CM, Zhang Y (2019) LES for pedestrian level wind around an idealized building array—assessment of sensitivity to influencing parameters. Sustain Cities Soc 44:406–415. https://doi.org/10.1016/j.scs.2018.10.034
144. Gousseau P, Blocken B, Van Heijst GJF (2013) Quality assessment of large-eddy simulation of wind flow around a high-rise building: validation and solution verification. Comput Fluids 79:120–133. https://doi.org/10.1016/j.compfluid.2013.03.006
145. Jiménez J, Moser RD (2000) Large-eddy simulations: where are we and what can we expect? AIAA J 38:605–612. https://doi.org/10.2514/2.1031
146. Sayadi T, Moin P (2012) Large eddy simulation of controlled transition to turbulence. Phys Fluids 24:114103. https://doi.org/10.1063/1.4767537
147. Choi H, Moin P (2012) Grid-point requirements for large eddy simulation: Chapman's estimates revisited. Phys Fluids 24:011702. https://doi.org/10.1063/1.3676783
148. Kempe T, Hantsch A (2017) Large-eddy simulation of indoor air flow using an efficient finite-volume method. Build Environ 115:291–305. https://doi.org/10.1016/j.buildenv.2017.01.019
149. Bazdidi-Tehrani F, Masoumi-Verki S, Gholamalipour P, Kiamansouri M (2019) Large eddy simulation of pollutant dispersion in a naturally cross-ventilated model building: comparison between sub-grid scale models. Build Simul 12:921–941. https://doi.org/10.1007/s12273-019-0525-5
150. Bazdidi-Tehrani F, Jadidi M (2014) Large eddy simulation of dispersion around an isolated cubic building: evaluation of localized dynamic kSGS-equation sub-grid scale model. Environ Fluid Mech 14:565–589. https://doi.org/10.1007/s10652-013-9316-1
151. Tominaga Y, Stathopoulos T (2010) Numerical simulation of dispersion around an isolated cubic building: model evaluation of RANS and LES. Build Environ 45:2231–2239. https://doi.org/10.1016/j.buildenv.2010.04.004
152. Xing F, Mohotti D, Chauhan K (2018) Experimental and numerical study on mean pressure distributions around an isolated gable roof building with and without openings. Build Environ 132:30–44. https://doi.org/10.1016/j.buildenv.2018.01.027
153. Schumann U (1975) Subgrid scale model for finite difference simulations of turbulent flows in plane channels and annuli. J Comput Phys 18:376–404. https://doi.org/10.1016/0021-9991(75)90093-5
154. Deardorff JW (1970) A numerical study of three-dimensional turbulent channel flow at large Reynolds numbers. J Fluid Mech 41:453–480. https://doi.org/10.1017/S0022112070000691

155. Spalart PR (2009) Detached-eddy simulation. Annu Rev Fluid Mech 41:181–202. https://doi.org/10.1146/annurev.fluid.010908.165130
156. Piomelli U, Rouhi A, Geurts BJ (2015) A grid-independent length scale for large-eddy simulations. J Fluid Mech 766:499–527. https://doi.org/10.1017/jfm.2015.29
157. Rouhi A, Piomelli U, Geurts BJ (2016) Dynamic subfilter-scale stress model for large-eddy simulations. Phys Rev Fluids 1:044401. https://doi.org/10.1103/PhysRevFluids.1.044401
158. Piomelli U, Ferziger J, Moin P, Kim J (1989) New approximate boundary conditions for large eddy simulations of wall-bounded flows. Phys Fluids A Fluid Dyn 1(1):1061–1068. https://doi.org/10.1063/1.857397
159. Werner H, Wengle H (1993) Large-eddy simulation of turbulent flow over and around a cube in a plate channel. In: Durst F, Friedrich R, Laund BE, Schmidt FW, Schumann U, Whitelaw JH (eds) Turbulent Shear flows 8. Springer, Berlin, p 155–168. https://doi.org/10.1007/978-3-642-77674-8_12
160. Temmerman L, Leschziner MA, Hanjalic K (2002) A-priori studies of a near-wall RANS model within a hybrid LES/RANS scheme. In: Proceedings of the 5th International Symposium on Engineering Turbulence Modelling and Measurements, Mallorca, 2002. p 317–326. https://doi.org/10.1016/B978-008044114-6/50030-2
161. Kawai S, Larsson J (2013) Dynamic non-equilibrium wall-modeling for large eddy simulation at high Reynolds numbers. Phys Fluids 25:015105. https://doi.org/10.1063/1.4775363
162. Patil S, Tafti D (2012) Wall modeled large eddy simulations of complex high Reynolds number flows with synthetic inlet turbulence. Int J Heat Fluid Flow 33:9–21. https://doi.org/10.1016/j.ijheatfluidflow.2011.09.010
163. Heinz S (2020) A review of hybrid RANS-LES methods for turbulent flows: concepts and applications. Prog Aerosp Sci 114:100597. https://doi.org/10.1016/j.paerosci.2019.100597
164. Spalart P, Allmaras S (1992) A one-equation turbulence model for aerodynamic flows. Paper presented at the 30th Aerospace Sciences Meeting and Exhibit, Reno. https://doi.org/10.2514/6.1992-439
165. Paik J, Sotiropoulos F (2010) Numerical simulation of strongly swirling turbulent flows through an abrupt expansion. Int J Heat Fluid Flow 31:390–400. https://doi.org/10.1016/j.ijheatfluidflow.2010.02.025
166. Viswanathan AK, Tafti DK (2006) Detached eddy simulation of turbulent flow and heat transfer in a two-pass internal cooling duct. Int J Heat Fluid Flow 27:1–20. https://doi.org/10.1016/j.ijheatfluidflow.2005.07.002
167. Viswanathan AK, Tafti DK (2006) A comparative study of DES and URANS for flow prediction in a two-pass internal cooling duct. J Fluids Eng 128:1336–1345. https://doi.org/10.1115/1.2353279
168. Viswanathan AK, Tafti DK (2007) Capturing effects of rotation in sudden expansion channels using detached eddy simulation. AIAA J 45:2100–2102. https://doi.org/10.2514/1.27429
169. Šarić S, Kniesner B, Mehdizadeh A, Jakirlić S, Hanjalić K, Tropea C (2008) Comparative assessment of hybrid LES/RANS models in turbulent flows separating from smooth surfaces. In: Peng SH, Haase W (eds) Advances in Hybrid RANS-LES Modelling. Notes on Numerical Fluid Mechanics and Multidisciplinary Design, vol 97. Springer, Berlin. https://doi.org/10.1007/978-3-540-77815-8_15
170. Strelets M (2001) Detached eddy simulation of massively separated flows. Paper presented at the 39th Aerospace Sciences Meeting and Exhibit, Reno. https://doi.org/10.2514/6.2001-879
171. Hu J, Xuan HB, Kwok KCS, Zhang Y, Yu Y (2018) Study of wind flow over a 6 m cube using improved delayed detached eddy simulation. J Wind Eng Ind Aerodyn 179:463–474. https://doi.org/10.1016/j.jweia.2018.07.003
172. Yan BW, Li QS (2017) Detached-eddy and large-eddy simulations of wind effects on a high-rise structure. Comput Fluids 150:74–83. https://doi.org/10.1016/j.compfluid.2017.02.009
173. Lateb M, Masson C, Stathopoulos T, Bédard C (2014) Simulation of near-field dispersion of pollutants using detached-eddy simulation. Comput Fluids 100:308–320. https://doi.org/10.1016/j.compfluid.2014.05.024
174. Liu J, Niu J (2016) CFD simulation of the wind environment around an isolated high-rise building: an evaluation of SRANS, LES and DES models. Build Environ 96:91–106. https://doi.org/10.1016/j.buildenv.2015.11.007
175. Liu J, Niu J (2019) Delayed detached eddy simulation of pedestrian-level wind around a building array – the potential to save computing resources. Build Environ 152:28–38. https://doi.org/10.1016/j.buildenv.2019.02.011
176. Liu J, Niu J, Mak CM, Xia Q (2017) Detached eddy simulation of pedestrian-level wind and gust around an elevated building. Build Environ 125:168–179. https://doi.org/10.1016/j.buildenv.2017.08.031
177. Mokhtarpoor R, Heinz S, Stoellinger M (2016) Dynamic unified RANS-LES simulations of high Reynolds number separated flows. Phys Fluids 28:095101. https://doi.org/10.1063/1.4961254
178. Balaras E, Benocci C (1994) Subgrid scale models in finite difference simulations of complex wall bounded flows. Paper presented at the 74th Fluid Dynamics Symposium on Application of Direct and Large Eddy Simulation to Transition and Turbulence, Chania
179. ESDU (2001) Characteristics of atmospheric turbulence near the ground. Part II: single point data for strong winds (neutral atmosphere). https://esdu.com/cgi-bin/ps.pl?sess=unlicensed_1220511003544gbs&t=doc&p=esdu_85020g
180. Lungu D, van Gelder P (1997) Characteristics of wind turbulence with applications to wind codes. In: Proceedings of the 2nd European & African Conference on Wind Engineering, Genova
181. Sadek F, Simiu E (2002) Peak non-Gaussian wind effects for database-assisted low-rise building design. J Eng Mech 128:530–539. https://doi.org/10.1061/(asce)0733-9399(2002)128:5(530)

Publisher's Note